anima

MDP

Article

Differential gene expression associated with soybean oil level in the diet of pigs

Simara Larissa Fanalli[1], Bruna Pereira Martins da Silva[1], Julia Dezen Gomes[2], Vivian Vezzoni de Almeida[3], Felipe André Oliveira Freitas[2], Gabriel Costa Monteiro Moreira[4], Bárbara Silva-Vignato[2], Juliana Afonso[5], James Reecy[6], James Koltes[6], Dawn Koltes[6], Luciana Correa Almeida Regitano[5], Dorian Garrick[7], Júlio Cesar de Carvalho Baileiro[8], Ariana Nascimento Meira[2], Luciana Freitas[8], Luiz Lehmann Coutinho[2], Heidge Fukumasu[1]; Gerson Barreto Mourão[2], Severino Matias de Alencar[2], Albino Luchiari Filho[2], and Aline Silva Mello Cesar[1,2]*

1. Faculty of Animal Science and Food Engineering, University of São Paulo, Pirassununga, São Paulo, Brazil.
2. Luiz de Queiroz College of Agriculture, University of São Paulo, Piracicaba, São Paulo, Brazil.
3. Federal University of Goiás, College of Veterinary Medicine and Animal Science, Goiânia, Goiás, Brazil.
4. University of Liège, GIGA Medical Genomics, Unit of Animal Genomics, Liège,
5. Embrapa Pecuária Sudeste, São Carlos, São Paulo, Brazil.
6. Iowa State University, College of Agriculture and Life Sciences, Ames, Iowa, USA;
7. AL Rae Centre for Genetics and Breeding, Massey University, Hamilton, New Zealand.
8. College of Veterinary Medicine and Animal Science, University of São Paulo, Pirassununga, São Paulo, Brazil.
8. DB Genética de Suínos, Patos de Minas, MG, Brazil.
* Correspondence: *E-mail address*: alinecesar@usp.br (A.S.M. Cesar)

Simple Summary: The analysis of the pig transcriptome, findings may help to better understand the biological mechanisms that can be modulated by the diet. Thus, the aim of this study was to identify the differentially expressed genes from the skeletal muscle and liver samples of pigs fed diets with two different levels of soybean oil (1.5 or 3%). The FA profile in the tissues was modified by the diet mainly related to MUFA and PUFA. In skeletal muscle, network maps related to inflammation and immune process were enriched, and pathways associated with the metabolic diseases. On the other hand, in liver tissue, the transcriptome analysis revealed network maps related dysfunction in neurodegenerative diseases. This nutrigenomics study verified the effect of different levels of soybean oil in the pig diet on the transcriptome profile of skeletal muscle and liver.

Abstract: The aim of this study was to identify the differentially expressed genes (DEG) from the skeletal muscle and liver samples of animal model for metabolic diseases in human. To perform the study, the fatty acid (FA) profile and RNA sequencing (RNA-Seq) data of 35 samples of liver tissue (SOY1.5, n=17 and SOY3.0, n=18) and 36 samples of skeletal muscle (SOY1.5, n=18 and SOY3.0, n=18) of Large White pigs were analyzed. The FA profile of the tissues was modified by the diet, mainly those related to monounsaturated (MUFA) and polyunsaturated (PUFA) FA. The skeletal muscle transcriptome analysis revealed 45 DEG (FDR 10%), and the functional enrichment analysis identified network maps related to inflammation, immune process, and pathways associated with the oxidative stress, type 2 diabetes and metabolic dysfunction. For the liver tissue, the transcriptome profile analysis revealed 281 DEG, which participate in network maps related to neurodegenerative diseases. With this nutrigenomics study, we verified that different levels of soybean oil in the pig diet, an animal model for metabolic diseases in humans, affected the transcriptome profile of skeletal muscle and liver tissue. These findings may help to better understand the biological mechanisms that can be modulated by the diet.

Keywords: fatty acid, RNAseq, transcriptome, immune response, Huntington's disease, metabolism, hepatic tissue, *Longissimus lomborum*, biomedical model.

.

1. Introduction

The World Health Organization [1] estimated that 41 million people died in 2018 due to chronic non-communicable diseases (NCDs) including cardiovascular diseases (CVDs), cancers, and metabolic diseases such as type 2 diabetes, obesity, and neurodegenerative diseases. These diseases have in common the influence of genetic factors, oxidative stress, and inflammation as result of sedentary lifestyle, diet, and consumption of drugs and alcohol. Pigs have been used as a biomedical model for diseases and in nutrigenetics and nutrigenomics [2–5].

Metabolic diseases are any of the diseases or disorders that disrupt the normal process of converting food to energy into the cell, which involves the activity of thousands of enzymes. Among the metabolic processes that occurs into the cell are the process and transport of the proteins, carbohydrates, lipids, and their small organic molecules such as amino acids, sugars and starches, and fatty acids (FA), respectively [6,7].

The main process that generates energy is the cellular respiration that uses organic molecules (sugar and lipids) and oxygen. Part of the oxygen used in this process is transformed into superoxide or reactive oxygen species (ROS) that can cause harm to cells, tissues and organ [7]. Free radicals such as ROS are a highly toxic and reactive molecules capable of transforming other molecules such as proteins, lipids, and nucleic acids (DNA and RNA). This transformation changes the chemical structure and biological function of these molecules, disrupting the normal cellular metabolic processes and, as a consequence, leads to an inflammatory state and a pro-inflammatory immune response [6]

Meat has high nutritional importance and FA profile has impact on human health. Among its many benefits are its supply of unsaturated fatty acids, such as oleic acid (AO, C18:1 cis 9) and linoleic acid (AL, C18: 2 cis9, 12), which have positive effects on human health [8]. Pigs have been increasingly used in nutrigenomics research and for investigation of metabolic diseases in humans due to role as a biomedical model for humans (LUNNEY, 2007; BROWN; CORSON; CLARKE, 2010; MALGWI et al., 2022). Pigs are similarities in terms of anatomy, biochemistry, pathology, pharmacology and physiology with humans what makes them to be used as a biomedical model [4,9,11,12].

In pigs, the liver is a highly specialized organ, related to the regulation of several metabolic processes, along with the skeletal muscle, wich is essential for the regulation of lipid metabolism in mammals [13]. Muscle tissue is of fundamental importance in regulating lipid metabolism, which is regulated by various factors and molecules [14]. Free fatty acids are released from adipose tissue and enter skeletal muscle via intermembrane proteins. In addition, free fatty acids can regulate several genes and skeletal muscle lipogenesis, including Sterol regulatory-element binding proteins (*SREPB*), Nuclear factor kappa B (*NFkB*), liver X receptors, retinoid X receptors, receptors activated by peroxisome proliferators (*PPARs*) [14].

The characterization of gene networks involved in immune cell function and metabolism in health and disease is important to understand immunodeficiency or autoimmunity disorders caused by an unbalanced immune response ([15]. Dysfunctional peroxisomes result in overall lipid alterations, such as accumulation of very long-chain fatty acids (VLCFA) and VLCFA-cholesteryl esters [15]. Lipid metabolic dysregulation can cause inflammation, participating in the modulation of the immune system responses [15–17]. Furthermore, among the proteins that drive inflammation are cytokines that are previously secreted by immune cells and vascular endothelial cells [15,16].

Lipids are a major class of biological molecules, ubiquitously distributed in all types of cells. They regulate transcription, store energy, and contribute to many biological processes, such as cellular structure and energy storage [18]. FA are among the most important dietary components found in meat, which is rich in polyunsaturated (PUFA), saturated (SFA), and monounsaturated (MUFA) fatty acids (WOOD et al., 2008). Consumption of FA has been linked to metabolic effects, including altered blood parameters; such as lipid and lipoprotein composition [19]. Nevertheless, past studies and meta-analyses have noted contrasting opinions regarding the role of FA in animal and human health [20].

Our previous studies in different species revealed a significant number of genes differentially expressed between animals with divergent values of FA content in skeletal muscle, associated with biological processes such as insulin receptor signaling, activated T cell nuclear factors (NFAT) in cardiac hypertrophy, mitochondrial disorder, and neurodegenerative disorders such as Huntington's and Alzheimer's disease (AD). The study shows that fatty acids have a significant impact on gene expression associated with important biological processes, such as oxidative phosphorylation, cell growth, survival, and migration [21].

Human consumption of MUFA and PUFA has been related with low levels of low-density lipoprotein (LDL) and with potentially increased levels of high-density lipoprotein (HDL) in the blood. Pig meat has a high unsaturation fatty acid profile, mainly due to oleic acid (OA), and plays a significant role in human nutrition and health [22–25]. Another important aspect of unsaturated FA content is the relationship with meat quality characteristics, such as juiciness, flavor, and shelf life [26]. In the context of improving our knowledge about the biological processes associated with FA content in different tissues, scientific studies of this kind are extremely important. This knowledge can be applied both in animal production (genetic improvement, nutrition, and environment) as in animal and human health.

Pig diets added with vegetable oils rich in unsaturated fatty acids can be a source of healthier products for consumers [27]. Thus, vegetable oils such as canola, sunflower and soybean oil are interesting options due to the amount of PUFA [28]. On the other hand, there is a need to fill in the knowledge gaps regarding the impact of the amount of soybean oil added on gene expression and the functional and nutritional knowledge of lipids. Thus, our hypothesis is that different levels of soybean oil (1.5% *vs* 3%) added in the diet of Large White pigs can affect the variation in the fatty acid profile deposition could be associated with gene expression profile of the skeletal muscle and liver tissue of these animals, modulating biological processes involved with lipid metabolism and metabolic diseases.

The present study aimed to (1) evaluate changes in fatty acid profile and gene expression of the skeletal muscle and liver tissue of pigs fed a diet with different levels of soybean oil; (2) identify metabolic pathways and gene networks impacted by the dietary fatty acid composition of the pigs' tissues that were fed with different proportions of degummed soybean oil.

2. Materials and Methods

2.1. Ethics statement

All procedures involving animals were approved by the Animal Care and Use Committee of Luiz de Queiroz College of Agriculture (University of São Paulo, Piracicaba, Brazil, protocol: 2018.5.1787.11.6 and number CEUA 2018-28) and followed ethical principles in animal research, according to the Guide for the Care and Use of Agricultural Animals in Agricultural Research and Teaching [29].

2.2. Animals

In our 98-day feeding study, thirty-six genetically lean immunocastrated male pigs (offspring of Large White sires x Large White dams) with an average initial body weight (BW) of 28.44 ± 2.95 kg and an average age of 71 ± 1.8 days were used. All the animals were genotyped for the halothane mutation (RYR1 gene) according to Fujii et al. [30]; thus, pigs selected for this trial were all halothane homozygous-negative (NN). The animals were randomly allotted to one of two dietary treatments with six replicate pens per treatment and three pigs per pen, which were housed in an all-in/all-out double-curtain-sided building. Each pen was equipped with a three-hole dry self-feeder and a nipple drinker, allowing pigs ad libitum access to feed and water throughout the experimental period. Immunocastration of the intact males was performed by the administration of two 2-mL dose of Vivax® (Pfizer Animal Health, Parkville, Australia) on day 56 (127 days of age) and day 70 (141 days of age) [31,32], in accordance with the manufacturer's recommendations.

As discussed in our previous works, the experimental diet consisted in a six-phase diet that was as follows: two in the grower and four for finisher. Dietary treatments consisted of corn-soybean meal growing-finishing diets supplemented with 1.5% soybean oil (SOY1.5, common level used in commercial pig production) or 3% soybean oil (SOY3.0). The diets were formulated to reach or exceed Rostagno et al. [33] recommendations for growing-finishing pigs. The diets were formulated to have a similar level of digestible energy. No antibiotic growth promoters were used, and all diets were provided in a mash meal form [31].

2.3. Fatty acid profile

Sample collection fatty acid profile was previously described in Almeida et al., [31], and Fanalli et al., [32]. In summary, liver and skeletal muscle (*Longissimus lumborum*) samples were collected, and then stored at -80 °C until fatty acid profile and RNA sequencing analyses. The FA profile was performed by Bligh and Dyer [34] and methylated according to the procedure outlined by AOCS, (2005) (Method AM 5-04).

Statistical analyzes to verify differences in the FA profile of skeletal muscle and liver tissue between the diets were performed using the "proc mixed" procedure of the SAS statistical software (v. 9.4), where the mixed model was adopted using the restricted maximum likelihood (REML) methodology. In the model, the block effects were declared as a random effect and the treatments as a fixed effect. A normal distribution of the data was assumed and exploratory analyzes were performed previously to verify the consistency of the data. The SAS "proc univariate" procedure (v. 9.4) was used to verify the fit of the normal distribution and homogeneity of residuals for each of the variables. Diagnostics of the density distribution of the Studentized Residual of the model were made with the Shapiro-Wilk test and also, graphs were plotted as a histogram with normal density, Scatterplot and "QQ plot" for visual analysis of the dispersion of residues with the option "residual" of the "mixed proc" (SAS v.9.4).

2.4. Tissue RNA extraction and RNA-sequencing

Total RNA was extracted from skeletal muscle and liver tissue samples using commercial RNA extraction kits (RNeasy® Mini Kit, Qiagen), according to the manufacturer instructions. With the spectrophotometer Nanodrop 1000 and Bioanalyzer, RNA quantification, purity and integrity were evaluated, respectively. All samples presented an RNA Integrity Number (RIN) higher or equal to seven. From the total RNA from each sample, 2µg were used for library preparation according to the protocol described in the TruSeq RNA Sample Preparation kit v2 guide (Illumina, San Diego, CA). The estimation of libraries average size was made with the Agilent

Bioanalyzer 2100 (Agilent, Santa Clara, CA, USA) and the libraries were quantified using quantitative PCR with the KAPA Library Quantification kit (KAPA Biosystems, Foster City, CA, USA). Quantified samples were diluted and pooled (five pools of all 36 samples each), using TruSeq DNA CD Index Plate (96 indexes, 96 samples, Illumina, San Diego, CA, USA). All samples are pooled and sequenced in five lanes of a sequencing flowcell, using the TruSeq PE Cluster kit v4-cBot-HS kit (Illumina, San Diego, CA, USA), were clustered and sequenced using HiSeq2500 equipment (Illumina, San Diego, CA, USA) with a TruSeq SBS Kit v4-HS (200 cycles), according to manufacturer instructions. All the sequencing analyses were performed at the Genomics Centre at ESALQ, localized in the Animal Biotechnology Laboratory at ESALQ – USP, Piracicaba, São Paulo, Brazil [21].

Sequencing adaptors and low complexity reads were removed in an initial data filtering step by Trim Galore 0.6.5 software. Phred score lower than 33; only the reads with a length higher than 70 nucleotides were kept after trimming. Quality control and reads statistics were estimated with FASTQC version 0.11.8 software [http://www.bioinformatics.bbsrc.ac.uk/projects/fastqc/]. *Sus Scrofa 11.1* reference assembly available at Ensembl [http://www.ensembl.org/Sus_scrofa/Info/Index]. The abundance (read counts) of mRNAs for all annotated genes was calculated using STAR-2.7.6a [http://bioinformatics.oxfordjournals.org/content/29/1/15].

2.5. Data analysis, differentially expressed genes, and functional enrichment analysis

Differentially expressed genes (DEG) between the two different diets (SOY1.5 and SOY3.0) from skeletal muscle and liver tissue were identified using the DESeq2 available at Bioconductor open-source software for bioinformatics, using a multi-factor design [36] statistical package in R. Prior to statistical analysis the read count data was filtered as follows: i) genes with zero counts for all samples, that is, unexpressed genes, ii) genes with less than one read per sample on average were removed (very lowly expressed); iii) genes that were not present in at least 50% of the samples were removed (rarely expressed). Sire was fit as factor in the multi-factor model. The cut-off approach performed to identify the DEG was control the false discovery rate (FDR) at 10% [21], by using the Benjamini- Hochberg [37] methodology.

For skeletal muscle the functional enrichment analysis by MetaCore [38] was applied to identify the pathway maps from 45 DEG, and in the liver 281 DEG using. The functional enrichment analysis of DEG (FDR <0.10) was performed to obtain comparative networks by 'analyze single experiment' using a standard parameter of MetaCore software v.22.1 build 70800 using *Homo sapiens* genome annotation as background reference and a default parameter. The filters used were metabolic maps: energy metabolism, lipid metabolism, steroid metabolism; cardiovascular diseases: atherosclerosis; regulation of metabolism; nutritional and metabolic diseases, and nervous system diseases. To understand the behavior of genes and their interactions, gene networks were created using the Process Networks tool in MetaCore.

3. Results

3.1. Fatty acid profile for skeletal muscle and liver tissue

To analyze the changes in FA profiles, we identified the FA composition in the tissues, resulting in lipidic profile changes in skeletal muscle and liver of growing and finishing pigs receiving a diet enriched with different proportions of soybean oil.

The *Longissimus lumborum* intramuscular fat composition (Table 1) was modified with the increase in the proportion of oil to C18:1 n-9) (*p*-value <0.01), that is, with the increase in dietary oil, FA deposition increased.

Table 1: Effects of dietary treatments on fatty acid profile of *Longissimus lumborum* intramuscular fat of pigs

| Fatty Acid (%) | Dietary treatment | | | |
	SOY1.5	SOY3.0	Pooled SEM[2]	*p-value*
Saturated fatty acid (SFA)				
Myristic acid (C14:0)	1.14	1.19	0.04	0.20
Palmitic acid (C16:0)	25.50	25.01	0.21	0.21
Stearic acid (C18:0)	12.18	11.89	0.15	0.42
Monounsaturated fatty acid (MUFA)				
Palmitoleic acid (C16:1)	2.86	3.17	0.13	0.02
Eicosenoic acid (C20:1)	0.51	0.55	0.03	0.11
Oleic acid (C18:1 n-9)	38.93	44.15	1.40	<0.01
Polyunsaturated fatty acid (PUFA)				
Linoleic acid (C18:2 n-6)	17.90	13.28	1.12	<0.01
Alpha-linolenic acid (C18:3 n-3)	0.77	0.56	0.06	<0.01
Eicosapentaenoic acid (C20:5 n-3)	0.30	0.15	0.09	0.12
Docosahexaenoic acid (C22:6 n-3)	0.36	0.16	0.08	0.03
Total SFA	38.83	38.09	0.65	0.26
Total MUFA	42.29	47.70	1.48	<0.01
Total PUFA	19.28	14.80	1.72	0.02
Total n-3 PUFA[3]	1.35	0.87	0.15	<0.01
Total n-6 PUFA[4]	17.90	13.28	1.12	<0.01
PUFA:SFA ratio[5]	0.50	0.39	0.05	0.03
n-6:n-3 PUFA ratio[6]	14.20	17.29	1.70	0.10
Atherogenic index	0.49	0.48	0.09	0.43

[1]Pigs (*n* = 36) were fed either a corn-soybean meal diet containing 1.5% soybean oil (SOY1.5) or diet containing 3% soybean oil (SOY3.0). Values represent the least square means from a subset of pigs (*n*= 36; 18 pigs/treatment).
[2]SEM = standard error of the least square means.
[3]Total n-3 PUFA = {[C18:3 n-3] + [C20:5 n-3] + [C22:6 n-3]}.
[4]Total n-6 PUFA = C18:2 n-6.
[5]PUFA:SFA ratio = total PUFA/total SFA.
[6]Σ n-6/Σ n-3 PUFA ratio.

In addition, the composition of the FA profile was also performed in the liver. The FA profile in the liver (Table 2) presented a different pattern as of the observed in the skeletal muscle in relation to the SFA as the C14:0 and C16:0 that presented differences (*p*-value <0.01) with high percentage in the samples from animals that received a diet enriched with 3% of oil, what can be due to the increase in Palmitic and Myristic acid. The C18:0 presented a higher content in samples from animals with the diet enriched in SOY1.5 (*p*-value <0.01). As it occurred in muscle, high values of OA were identified in

liver, C18:2 n-6 (*p*-value <0.01) was higher in SOY1, and C18:3 n-3 did not present difference between diets (*p*-value =0.07). The C22:6 n-3 presented a difference in intramuscular fat (*p*-value =0.03) and not in liver (*p*-value =0.11). The atherogenic index was lower in SOY1.5 compared to SOY3.0 (*p*-value <0.01).

Table 2: Effects of dietary treatments on fatty acid profile of liver tissue of pigs

Fatty acid (%)	Dietary treatment		Pooled SEM[2]	*p-value*
	SOY1.5	SOY3.0		
Saturated fatty acid (SFA)				
Myristic acid (C14:0)	0.73	0.98	0.05	<0.01
Palmitic acid (C16:0)	20.92	22.98	0.40	<0.01
Stearic acid (C18:0)	25.48	21.28	1.06	<0.01
Monounsaturated fatty acid (MUFA)				
Palmitoleic acid (C16:1)	0.66	0.93	0.05	<0.01
Oleic acid (C18:1 n-9)	21.36	27.84	1.06	<0.01
Polyunsaturated fatty acid (PUFA)				
Linoleic acid (C18:2 n-6)	27.02	23.64	0.67	<0.01
Alpha-linolenic acid (C18:3 n-3)	1.42	1.17	0.10	0.07
Eicosapentaenoic acid (C20:5 n-3, EPA)	0.58	0.27	0.11	0.04
Docosahexaenoic acid (C22:6 n-3, DHA)	1.18	0.99	0.11	0.17
Total SFA	46.69	45.24	1.03	0.31
Total MUFA	22.01	28.78	1.04	<0.01
Total PUFA	30.79	26.06	0.55	<0.01
Total n-3 PUFA[3]	3.75	2.42	0.37	<0.01
Total n-6 PUFA[4]	27.02	23.64	0.67	<0.01
PUFA:SFA ratio[5]	0.67	0.58	0.02	<0.01
n-6:n-3 PUFA ratio[6]	8.51	9.90	0.50	0.05
Atherogenic index	0.42	0.51	0.01	<0.01

[1]Pigs (*n* = 35) were fed either a corn-soybean meal diet containing 1.5% soybean oil (SOY1.5) or diet containing 3% soybean oil (SOY3.0). Values represent the least square means from a subset of pigs (*n*= 35; 17pigs/SOY1.5; 18 pigs/SOY3.0).
[2]SEM = standard error of the least square means.
[3]Total n-3 PUFA = {[C18:3 n-3] + [C20:5 n-3] + [C22:6 n-3]}.
[4]Total n-6 PUFA = C18:2 n-6.
[5]PUFA:SFA ratio = total PUFA/total SFA.
[6]Σ n-6/Σ n-3 PUFA ratio.

3.2. Sequencing data and differential expression analysis

Thus, 36 samples (SOY1.5*vs*SOY3.0) of skeletal muscle and 35 samples (17 of SOY1.5 and 18 of SOY3.0) of liver tissue were used in subsequent RNA sequencing (RNA-Seq) data analysis. The total average number of sequenced reads before and after filtering for samples from the skeletal muscle of SOY1.5 group was 33,459,142 and 32,965,842, and of SOY3.0 group were 31,955,613 e 31,491,236. The total average number of reads before and after filtering for samples from liver tissue of the SOY1.5 group was

33,561,721 and 33,072,908, and of the SOY3.0 group were 34,078,903 e 33,610,858. On average, 78.59% of the total read pairs were uniquely mapped against the *Sscrofa11.1* reference genome assembly (Table S1) for both tissues and for each treatment.

Differential gene expression analysis was performed for each tissue by comparing gene expression levels between the two groups of animals that were fed with diets enriched with different levels of soybean oil (SOY1.5*vs*SOY3.0). A total of 45 DEG (log2 fold change ≥1; ≤−1; FDR-corrected *p*-value < 0.10) were identified in the skeletal muscle between the two groups, where 35 were down-regulated (log2FC ranging from -5.8 to -0.41) and 10 up-regulated (log2FC ranging from 2.3 to 0.53) in the SOY1.5 group compared with the SOY3.0 (Table S2a). For liver tissue, a total of 281 DEG (log2fold-change ≥1; ≤−1; FDR-corrected *p*-value <0.10) were identified, where 129 were down-regulated (log2FC ranging from -3.0 to -0.20) and 152 up-regulated (log2FC ranging from 4.8 to 0.24) in the SOY1.5 group (Table S2b). The Figure S1 shows the Volcano plot of log2 fold change (x-axis) *vs* -log10FDR-corrected *p-value* (y-axis) for skeletal muscle (Figure S1A) and liver tissue (Figure S1B) from the differential gene expression analysis between comparison.

3.2. Common differentially expressed genes between skeletal muscle and liver tissue

From the total of DEG, six genes were common between the two comparisons, in the skeletal muscle and liver tissue (Table 3). The *CDK20* gene, identified as DEG both in the skeletal muscle and liver of pigs fed with different levels of soybean oil, showed a higher expression in the SOY1.5 group for both tissues (log2 fold change +1.04 in the skeletal muscle, and log2 fold change +0.98 in the liver). In the same way, the *CCDC90B* was less expressed in the SOY1.5 group for both tissues (log2 fold change -0.41, skeletal muscle, and log2 fold change -0.45, liver). The ENSSSCG00000022842 or *LOC100525692* also was less expressed in the SOY1.5 group in both skeletal muscle (log2 fold change -1.8) and liver (log2 fold change -2.1), and the same occurred for *ALG6* (log2 fold change -0.68, skeletal muscle, and log2 fold change -0.74, liver). Finally, the ENSSSCG00000051557 showed higher expression in the SOY1.5 group for both the skeletal muscle (log2 fold change +1.28) and liver (log2 fold change +1.36).

Table 3. Common differentially expressed genes between the two tissues comparisons, in the skeletal muscle and liver tissue of pigs fed with two different levels of soybean oil in the diet (1.5 % and 3.0 % of soybean oil).

Gene common	Description	Reference
ENSSSCG00000009578 Cyclin dependent kinase 20 (*CDK20)*	Cell cycle related kinase. Its expression is related to the activation of β-catenin-TCF signaling and cell cycle progression. Can activate cyclin-dependent kinase 2 which is related to cell growth.	[39] [40]
ENSSSCG00000014903 Coiled-coil domain containing 90B (*CCDC90B)*	Paralog of the MCUR1 gene (Mitochondrial Calcium Uniporter Regulator 1) which is related to	[40]

the Ca, cAMP and lipid signaling pathways.

ENSSSCG00000022842 LOC100525692	Protein encoding gene.	[40]
ENSSSCG00000022842 Alpha-1,3-Glucosyltransferase *(ALG6)*	Related to N-Linked Glycosylation.	[40]
ENSSSCG00000017914 Glycolipid Transfer Protein Domain-Containing Protein 2 *GLTPD2*	Participates in the transfer of glycolipids.	[40]
ENSSSCG00000051557	-	-

3.3. Functional enrichment analysis for skeletal muscle differential expression

Seven different pathway maps were detected (*p*-value <0.10), which are linked to the Fatty Aldehyde Dehydrogenase or Aldehyde Dehydrogenase Family 3 Member A2 *(AL3A2)*, Alpha-2-Glycoprotein 1, Zinc-Binding *(AZGP1)*, and T-Cell Surface Glycoprotein *(CD4)* genes (Table 4).

Table 4. Pathway maps by MetaCore software (*p*-value <0.10) from the list of differentially expressed genes (FDR 10%) in the skeletal muscle of pigs fed with two different levels of soybean oil in the diet

Pathway maps	*p-value*	DEG[1]
Fatty Acid Omega Oxidation	3,33E-02	*AL3A2*
Leukotriene 4 biosynthesis and metabolism	4,42E-02	*AL3A2*
TNF-alpha, IL-1 beta induces dyslipidemia and inflammation in obesity and type 2 diabetes in adipocytes	4,64E-02	*AZGP1*
Breakdown of CD4+ T cell peripheral tolerance in type 1 diabetes mellitus	5,39E-02	*CD4*
Triacylglycerol metabolism p.1	6,56E-02	*AL3A2*
Oxidative stress in adipocyte dysfunction in type 2 diabetes and metabolic syndrome X	6,99E-02	*AL3A2*
Peroxisomal branched chain fatty acid oxidation"	9,08E-02	*AL3A2*

[1] Differentially expressed genes (DEG).

The DEG *AL3A2* was present in five (Figure 1, S2, S3, S4 and S5) of the seven pathway maps identified, which encodes the AL3A2 enzyme In this study the *AL3A2* was less expressed in SOY1.5 group (log2 fold change -0.77).
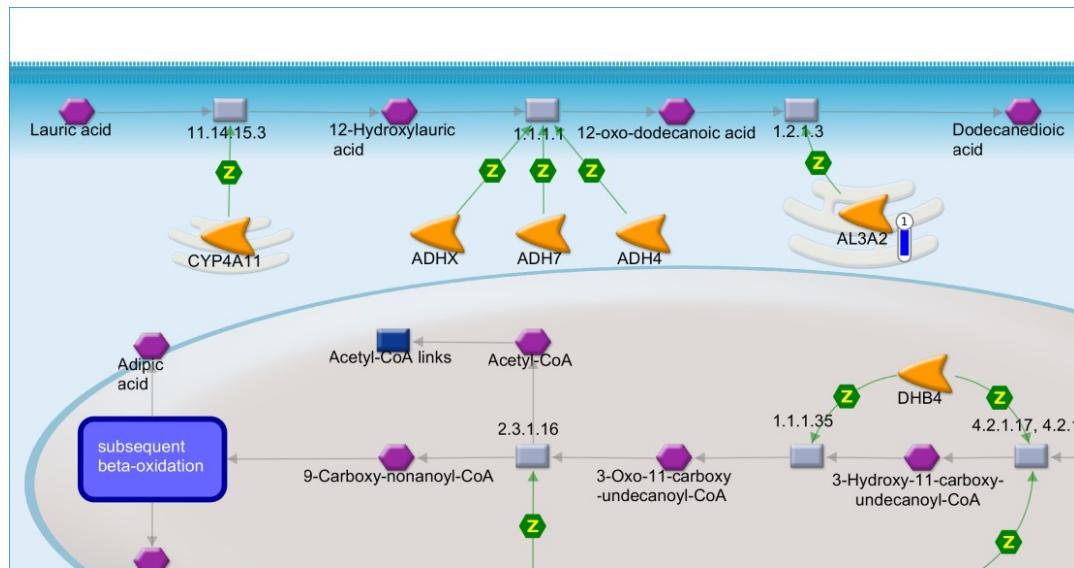
Figure 1. Fatty Acid Omega Oxidation pathway map created by using MetaCore software (p-value <0.10) and the list of differentially expressed genes (FDR 10%) in the skeletal muscle of fed with two different levels of soybean oil in the diet (1.5 % and 3.0 % of soybean oil). The blue thermometer indicates that the DEG is down-regulated (log2 fold change -0.77) in the diet with 1.5 % of soybean oil (SOY1.5). Green arrows indicate positive interaction and gray arrows indicates unspecified interaction. For a detailed definition, see https://portal.genego.com/legends/MetaCoreQuickReferenceGuide.pdf.

The *AZGP1* gene is involved in the *TNF-alpha* and *IL-1 beta (IL-1b)* pathways, which are involved with the occurrence of dyslipidemia and inflammation in adipocytes, leading to development of obesity and type 2 diabetes diseases (Figure 2). Herein, the *AZGP1* gene was less expressed in the SOY1.5 group (log2 fold change -2.67). Thus, the increase in soybean caused an increase in AZGP1 expression.log2 fold change Another DEG identified in this study was *CD4* enriched in the "breakdown of CD4+ T cell peripheral tolerance in type 1 diabetes mellitus" pathway in muscle (Figure 3), which was less expressed in SOY1.5 group (log2 fold change -1.57).
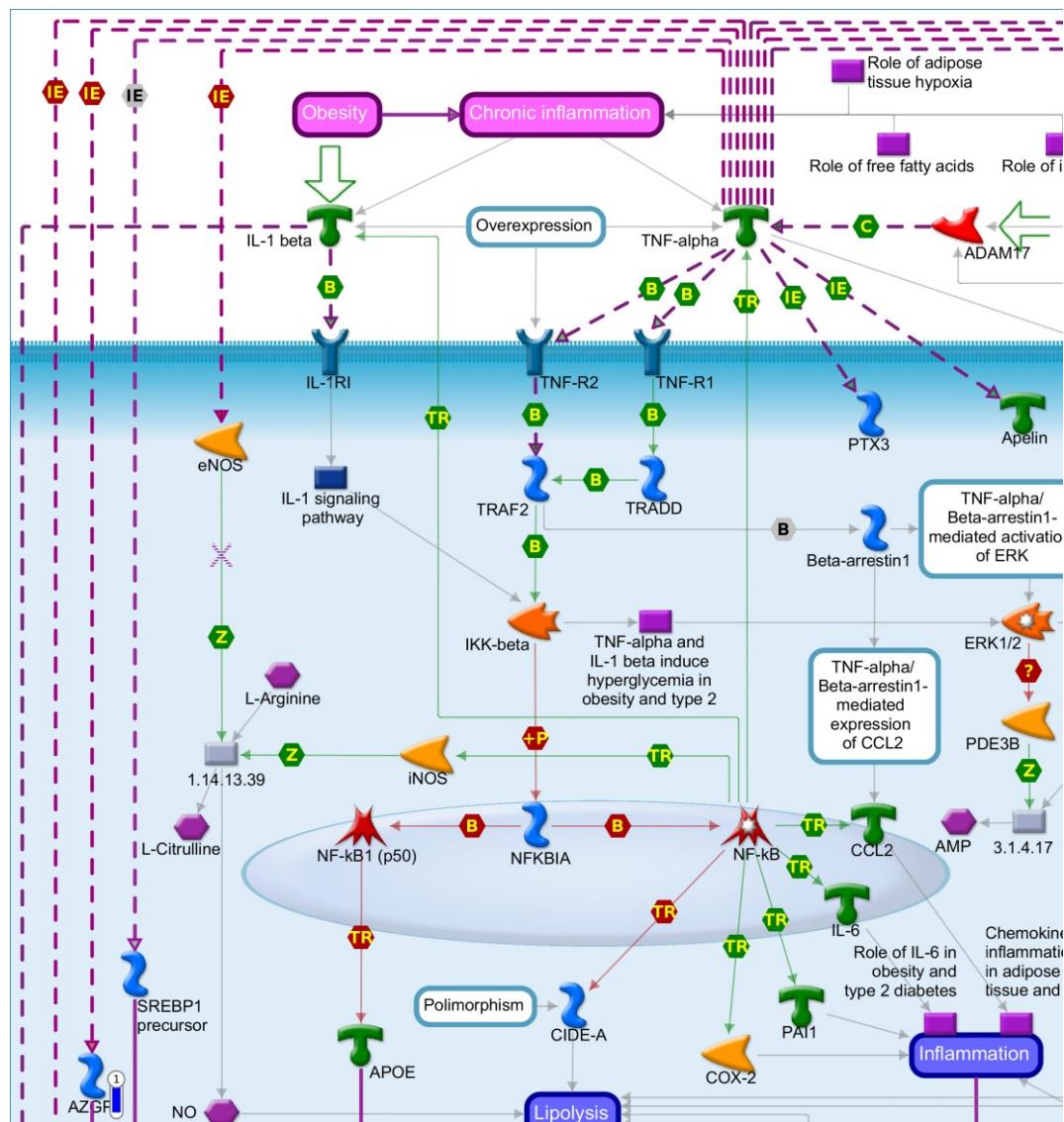
Figure 2. *TNF-alpha, IL-1 beta* induces dyslipidemia and inflammation in obesity and type 2 diabetes in adipocytes pathway map created by using MetaCore software (p-value <0.10) from the list of differentially expressed genes (FDR 10%) in the skeletal muscle of pigs fed with two different levels of soybean oil in the diet (1.5 % and 3.0 % of soybean oil). The blue thermometer indicates that the DEG is down-regulated (log2 fold change -2.67) in the diet with 1.5 % of soybean oil (SOY1.5). Purple lines indicates enhances in diseases and purple dotted line emerges in diseases. Green arrows indicates positive interactions, red arrows indicates negative interaction and gray arrows indicates unspecified interaction. For a detailed definition, see https://portal.genego.com/legends/MetaCoreQuickReferenceGuide.pdf.
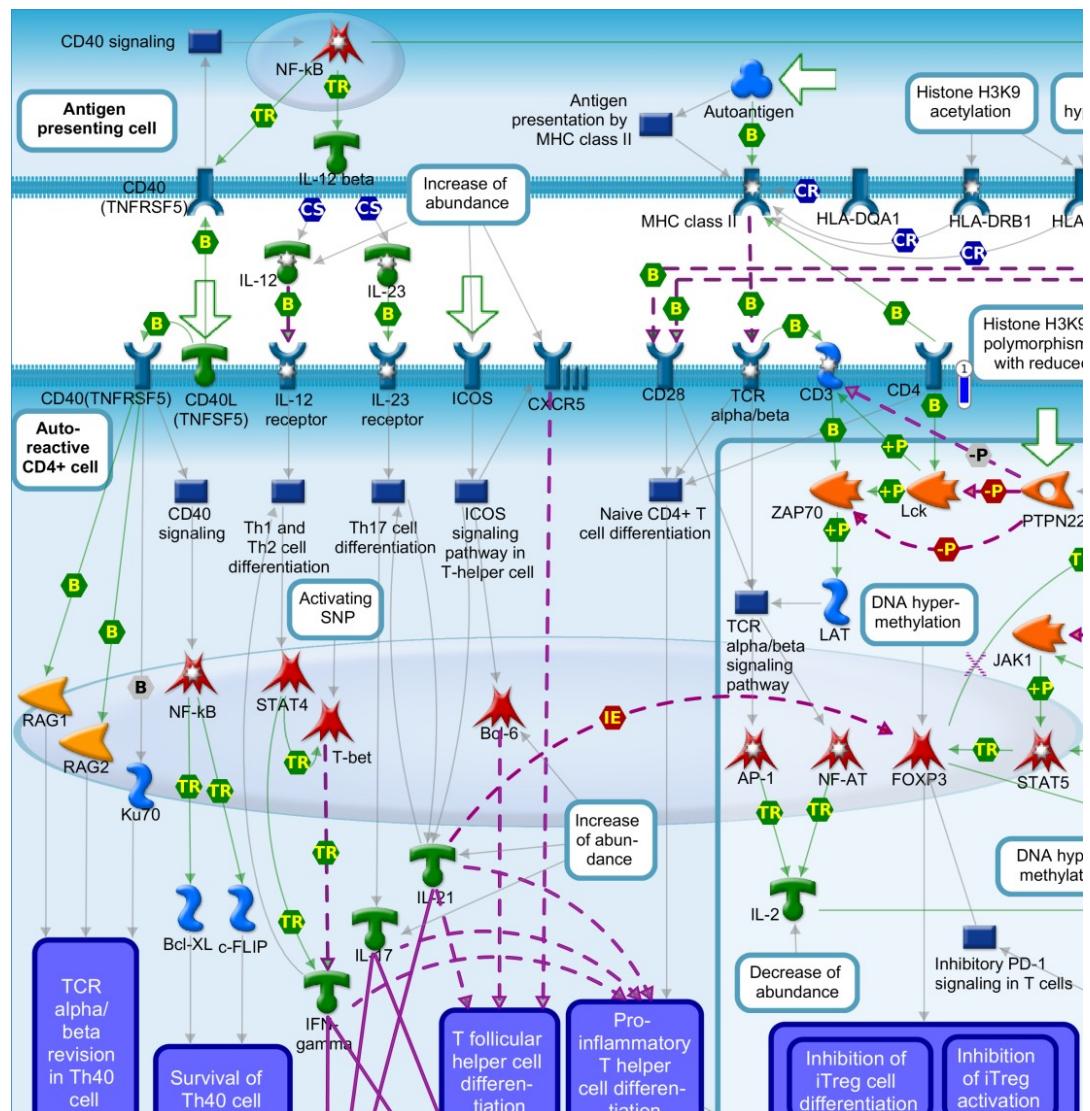
Figure 3: Breakdown of CD4+ T cell peripheral tolerance in type 1 diabetes mellitus pathway map created by MetaCore software (*p*-value <0.10) from the list of differentially expressed genes (FDR 10%) in the skeletal muscle of pigs fed with two different levels of soybean oil in the diet (1.5 % and 3.0 % of soybean oil). The blue thermometer indicates that the DEG is down-regulated (log2 fold change -1.57) in the diet with 1.5 % of soybean oil (SOY1.5). Purple lines indicates enhances in diseases and purple dotted line emerge in diseases. Green arrows indicates positive interactions, red arrows indicates negative interaction and gray arrows indicates unspecified interaction. For a detailed definition, see https://portal.genego.com/legends/MetaCoreQuickReferenceGuide.pdf.

The enriched pathways show our DEG identified by DESeq2 with an important role in metabolism and diseases (Table 5). The majority of the top 10 enriched *(p*-value < 0.05) processs networks identified are associated with immune response, the same observed in the pathway maps. The identified networks; such as, "immune response antigen presentation" with the DEG *AZGP1* and *CD4* (log2 fold change -2,67; log2 fold change -1.57), and "Kallikrein- kinin system" with the DEG *A2M* (alpha-2-macroglobulin; log2 fold change -1,79), are shown in Figures 4 and 5.

Table 5. Process Networks by MetaCore software (*p*-value <0.10) from the list of differentially expressed genes (FDR 10%) in the skeletal muscle of pigs fed with two different levels of soybean oil in the diet

Process Networks	*p-value*	DEG[1]
Chemostaxis	1,80E-03	*CCR10, GPCRs, CD4*
Cell adhesion_Leucocyte chemostaxis	3,78E-03	*CCR10, GPCRs, CD4*
Immune response_Antigen presentation	4,60E-03	*CD4, AZGP1*
Signal transduction_Leptin signaling	1,56E-02	*A2M, T-A2MG*
Inflammation_Kallikrein-kinin system	4,43E-02	*A2M, T-A2MG*
Reproduction_Male sex differentiation	6,99E-02	*Tektin 1, AKAP3*

[1] Differentially expressed genes (DEG).
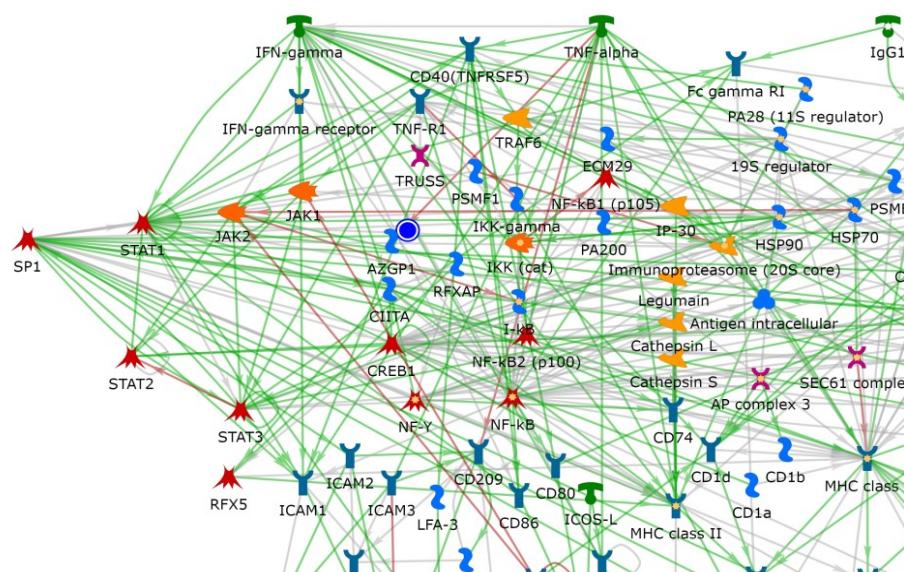
Figure 4. Process network Immune response antigen presentation identified by MetaCore software using the list of differentially expressed genes (FDR 10%) in the skeletal muscle of pigs fed with two different levels of soybean oil in the diet (1.5 % and 3.0 % of soybean oil). Green arrows indicates positive interactions, red arrows indicates negative interactions, and gray arrows indicates unspecified interactions. For a detailed definition, see https://portal.genego.com/legends/MetaCoreQuickReferenceGuide.pdf.
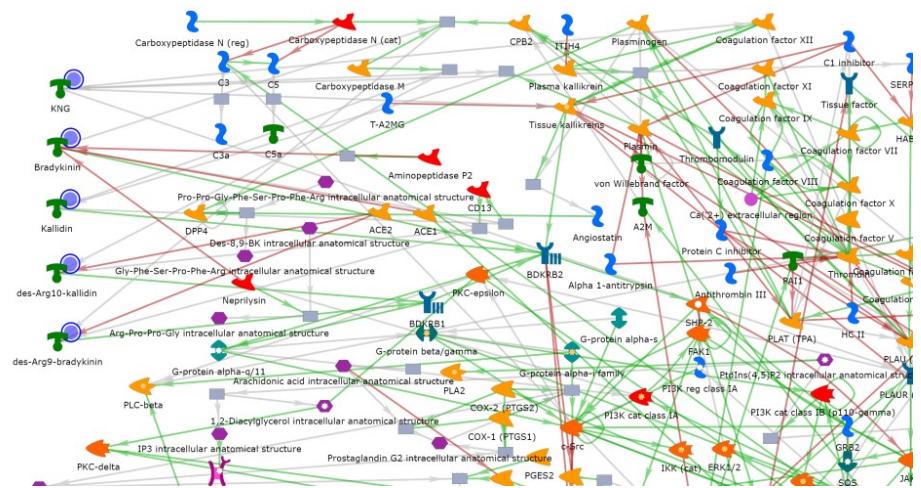
Figure 5. Process network Inflammation_Kallikrein-kinin system identified by MetaCore software using the list of differentially expressed genes (FDR 10%) in the skeletal muscle of pigs fed with two different levels of soybean oil in the diet (1.5 % and 3.0 % of soybean oil). Green arrows indicates positive interactions, red arrows indicates negative interactions and gray arrows indicates unspecified interactions. For a detailed definition, see https://portal.genego.com/legends/MetaCoreQuickReferenceGuide.pdf.

3.4. Functional enrichment analysis for liver differential expression

Six different pathway maps were detected (*p*-value <0.10), which are linked to BAG chaperone 1 *(BAG-1)*, *ST13* Hsp70 Interacting Protein (Hip), Microtubule Associated Protein Tau *(MAPT)*, group of non-phosphorylatable alkali light chains of Myosin II *(MELC)*, Protein Phosphatase 2 Catalytic *(PP2C)*, Adenine nucleotide translocases Protein group *(ANT)*, Peptidylprolyl Isomerase F *(PPIF)*, and cyclin dependent kinase inhibitor 1A *(CDKN1A ou p21)* genes (Table 6).

Table 6: Pathway maps with DEG between SOY1.5*vs*SOY3.0 in liver tissue enriched in significant pathways (*p*-value <0.10)

Pathway maps	*p-value*	DEG[1]
HSP70 and HSP40-dependent folding in Huntington's disease	1.034E-2	*BAG-1, ST13 (Hip)*
Inhibition of remyelination in multiple sclerosis: regulation of cytoskeleton proteins	3.022E-2	*MAPT, MELC*
Tau pathology in Alzheimer disease	4.543E-2	*MAPT, PP2C*
Mitochondrial dysfunction in neurodegenerative diseases	5.153E-2	*ANT*
Dual role of *p53* in transcription deregulation in Huntington's Disease	7.179E-2	*p21*
LRRK2 in neuronal apoptosis in Parkinson's disease	9.869E-.0.2	*ANT*

[1] Differentially expressed genes (DEG).

Herein, we identified the DEG *BAG-1* as an up-regulated gene (log2 fold change +0.35) in liver samples from pigs fed 1.5% of soybean oil. This gene participates in the pathway map named HSP70 and HSP40-dependent folding in Huntington's disease *BAG-1* (Figure 6).

We identified the *ST13* gene as a DEG in the liver of pigs that were fed with different levels of soybean oil (1.5% *vs* 3%), being less expressed in the SOY1.5 group (log2 fold change -0.35). In the "SP70 and HSP40-dependent folding in Huntington's disease" pathway ST13 is related to the folding process of mutant Huntington via stimulation of HSP70 (Figure 6).
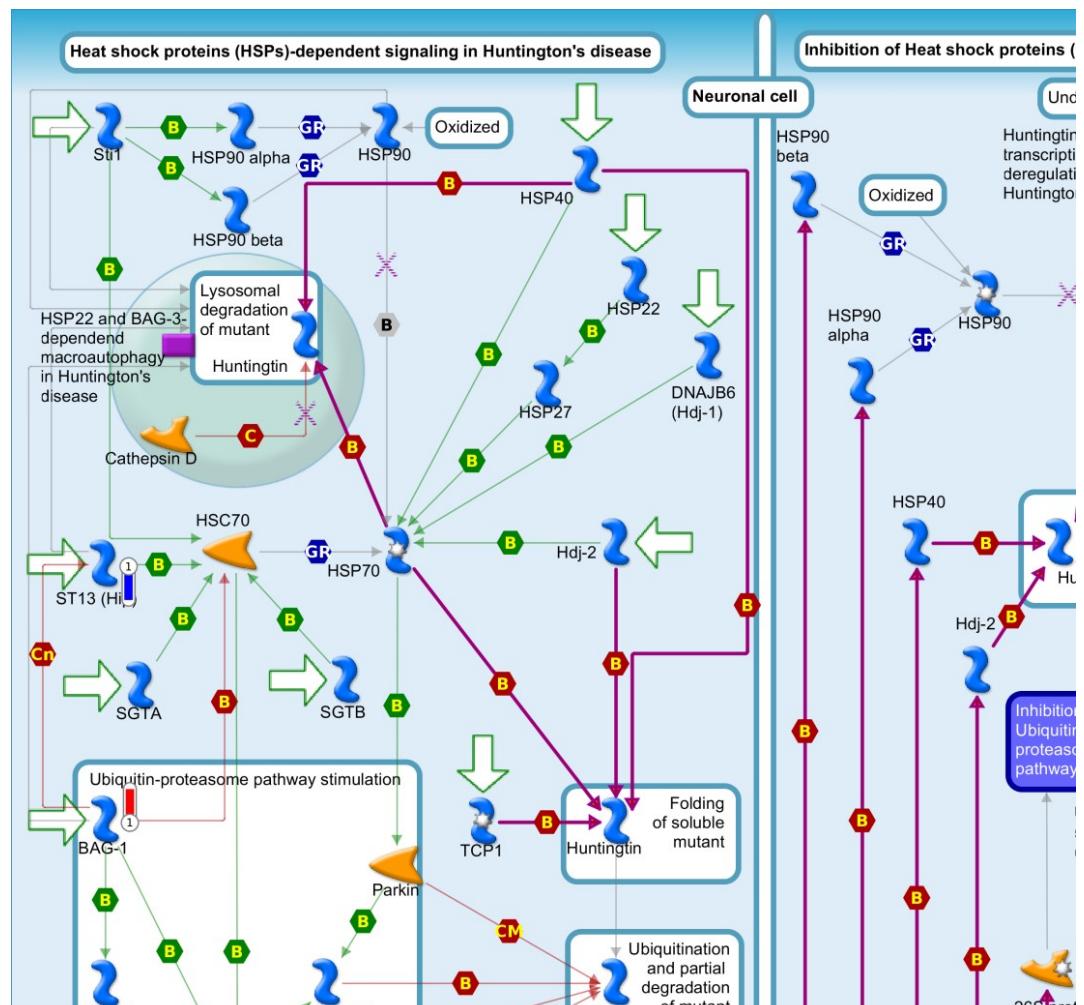
Figure 6. HSP70 and HSP40-dependent folding in Huntington's disease pathway map created by MetaCore software (*p*-value <0.10) and the list of differentially expressed genes (FDR 10%) in the liver of male pigs fed with two different levels of soybean oil in the diet (1.5 % and 3.0 % of soybean oil). The blue thermometer indicates that the DEG is down-regulated (log2 fold change -0.35) and the red thermometer indicates that the DEG is up-regulated (log2 fold change +0.35) in the diet with 1.5 % of soybean oil (SOY1.5). Purple lines indicates enhances in diseases and purple dotted line emerges in diseases. Green arrows indicates positive interactions, red arrows indicates negative interactions, and grey arrows indicates unspecified interactions. For a detailed definition, see https://portal.genego.com/legends/MetaCoreQuickReferenceGuide.pdf.

The microtubule associated protein *Tau (MAPT)* gene was identified as DEG in the liver of our pig population, showing lower expression (log2 fold change -1.18) in the SOY1.5 group and enriched in "Inhibition of remyelination in multiple sclerosis:

regulation of cytoskeleton proteins" (Figure 7) and "Tau pathology in Alzheimer disease" (Figure 8). Another interesting DEG identified herein, also enriched in the "inhibition of remyelination in multiple sclerosis: regulation of cytoskeleton proteins" pathway, was the Myosin light chain 3 (*MYL3*). The *MYL3* participates in the pathway as a MELC group with lower expression (log2 fold change -1.37) in SOY1.5 group.
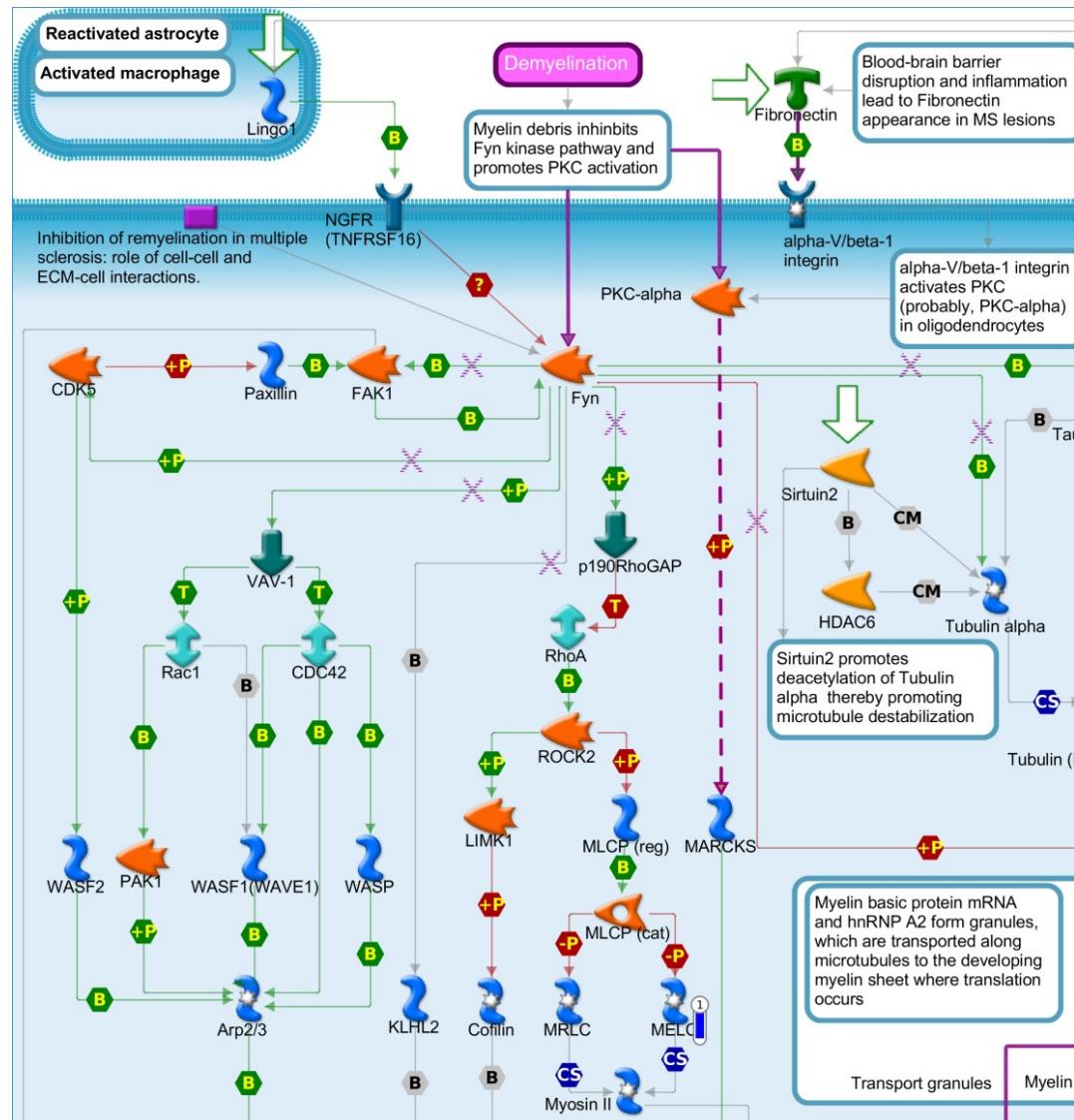

Figure 7. Inhibition of remyelination in multiple sclerosis: regulation of cytoskeleton proteins pathway map created by using MetaCore software (*p*-value <0.10) and the list of differentially expressed genes (FDR 10%) in the liver of pigs fed with two different levels of soybean oil in the diet (1.5 % and 3.0 % of soybean oil). The blue thermometer indicates that the DEG is down-regulated (log2 fold change -1.18 and -1.37) in the diet with 1.5 % of soybean oil (SOY1.5). Purple lines indicates enhances in diseases and purple dotted line emerges in diseases. Green arrows indicates positive interactions, red arrows indicates negative interactions and grey arrows indicates unspecified interactions. For a detailed definition, see https://portal.genego.com/legends/MetaCoreQuickReferenceGuide.pdf.
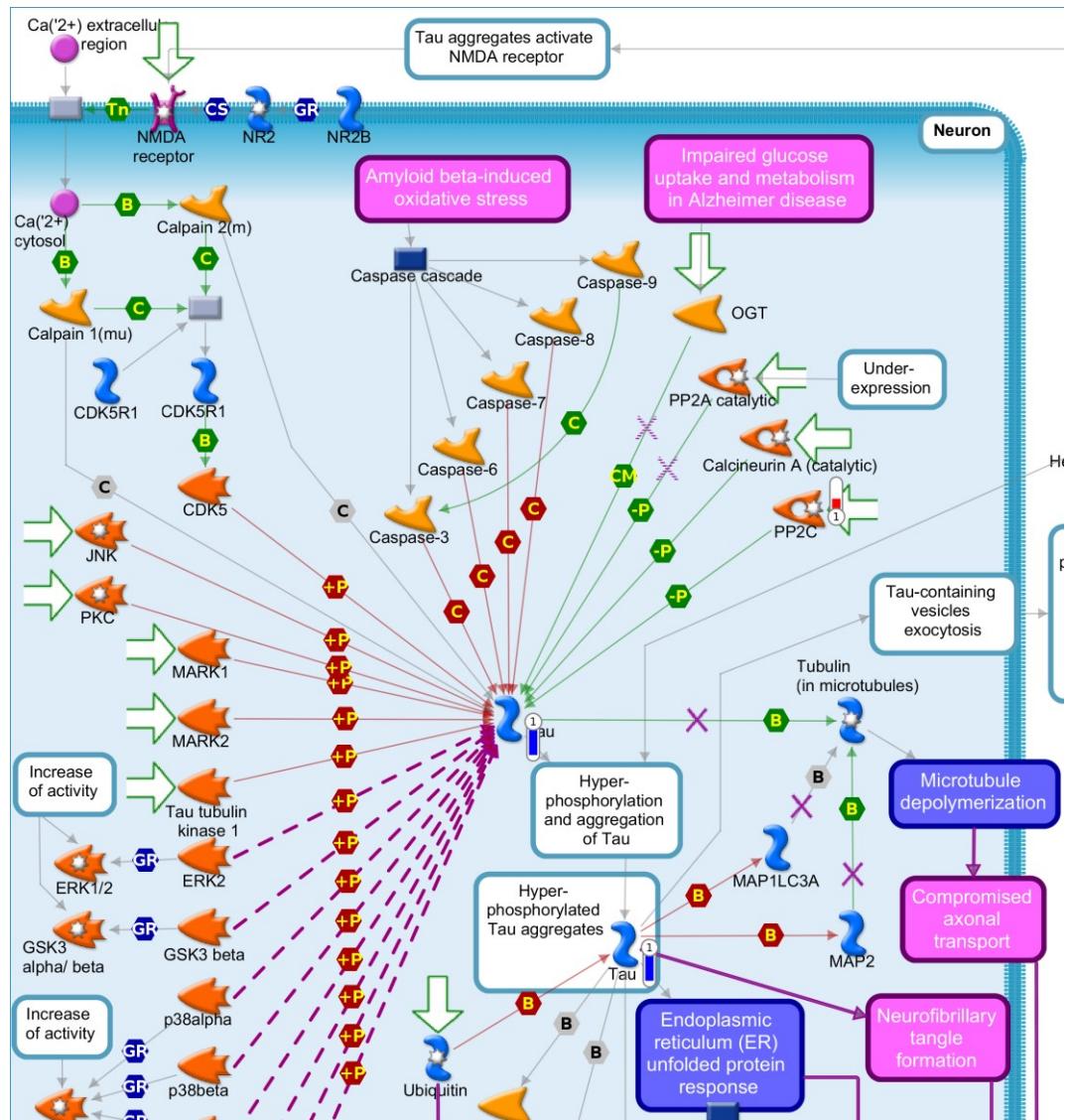
Figure 8. Tau pathology in Alzheimer disease pathway map created by using MetaCore software (*p*-value <0.10) and the list of differentially expressed genes (FDR 10%) in the liver of pigs fed with two different levels of soybean oil in the diet (1.5 % and 3.0 % of soybean oil). The blue thermometer indicates that the DEG is down-regulated (log2 fold change -1.18) and red thermometer indicates that the DEG is up-regulated (log2 fold change +0.42) in the diet with 1.5 % of soybean oil (SOY1.5). Purple lines indicates enhances in diseases and purple dotted line emerges in diseases. Green arrows indicates positive interactions, red arrows indicates negative interactions and grey arrows indicates unspecified interactions. For a detailed definition, see https://portal.genego.com/legends/MetaCoreQuickReferenceGuide.pdf.

The solute carrier family 25 member 4 *(SLC25A4)* gene was identified as DEG in liver of pigs that were fed with different levels of soybean oil (1.5 *vs* 3%), more expressed (log2 fold change +0.57) in the SOY1.5 group. The DEG *SLC25A5* was involved in the "mitochondrial dysfunction in neurodegenerative diseases" enriched pathway (Figure S6), as the adenine nucleotide translocases protein group (*ANT*).

Another gene identified as a DEG in liver of pigs that were fed with different levels of soybean oil (1.5 *vs* 3%) is the peptidylprolyl isomerase F (*PPIF*), member of the

peptidil-prolil cis-trans isomerase family *(PPIas*e), that was more expressed (log2 fold change +0.81) in the SOY1.5 group. In the Mitochondrial dysfunction in neurodegenerative disease pathway (Figure S6), the DEG *PPIF* is linked to the *ANT* gene.

The GO network pathways (*p*-value <0.10) were identified using the program's default in analyze single experiment (Figure 9).
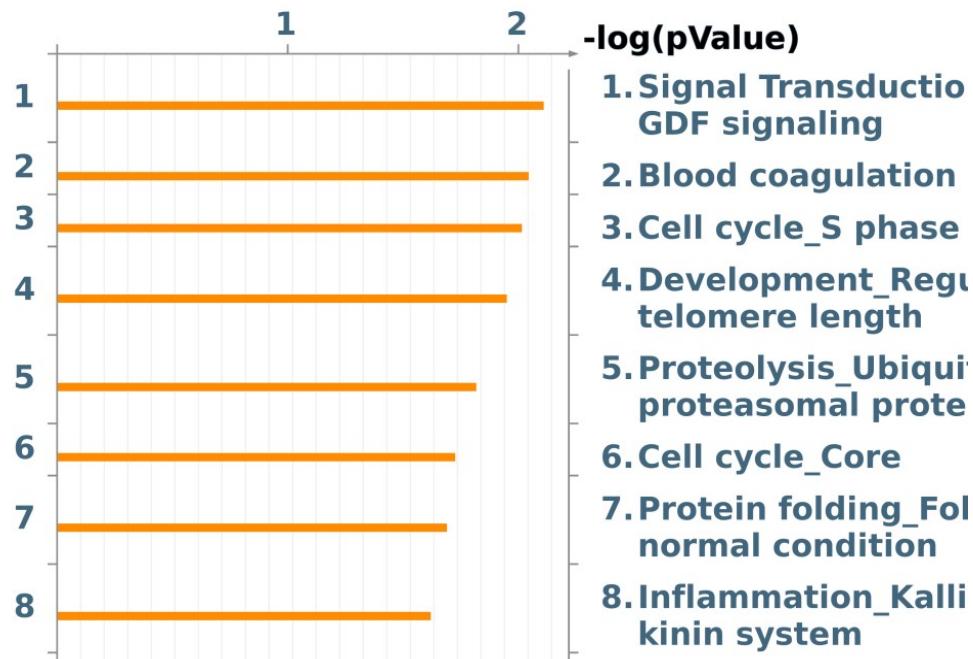

Figure 9. Top 10 enriched networks identified by MetaCore software from the list of differentially expressed genes (FDR 10%) in the liver of pigs fed with two different levels of soybean oil in the diet (1.5 % and 3.0 % of soybean oil).

The "protein folding in normal condition" network presents the DEG *PPID* (+0.48log2 fold change), HSP105 (+0.83log2 fold change), *BAG-1* (+0.35log2 fold change), and *ST13* (Hip) (-0.35log2 fold change) (Figure 10). The "inflammation_Kallikrein-kinin system", contains the DEG *KNG1* (-0.67log2 fold change), which in the gene network appears enriched as a receptor ligand, and has bioactive metabolites of bradykinin as can be seen in Figure 11 (within a blue circle).
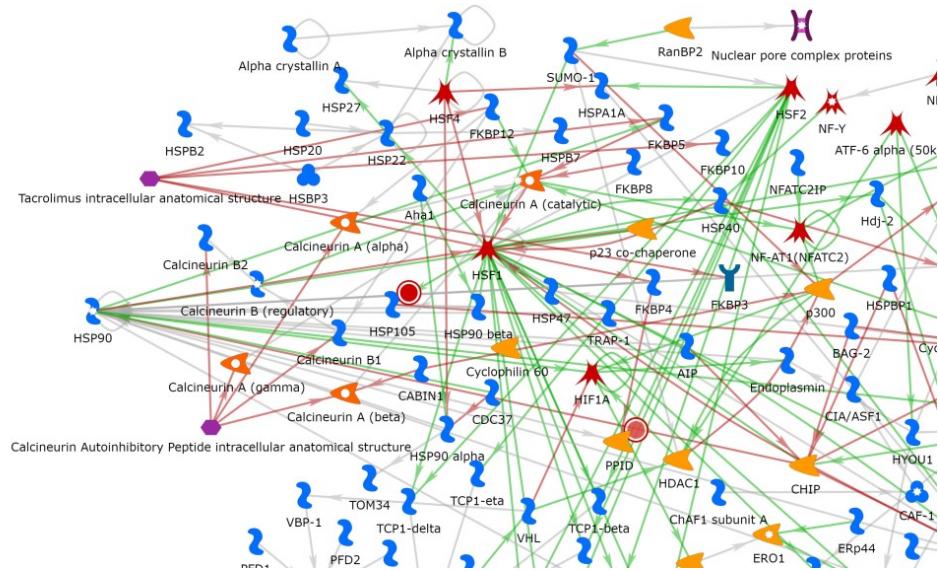
Figure 10. Process network Protein folding in normal condition identified by MetaCore software from the list of differentially expressed genes (FDR 10%) in the liver of pigs fed with two different levels of soybean oil in the diet (1.5 % and 3.0 % of soybean oil). Green arrows indicates positive interactions, red arrows indicates negative interaction and gray arrows indicates unspecified interaction. For a detailed definition, see https://portal.genego.com/legends/MetaCoreQuickReferenceGuide.pdf.
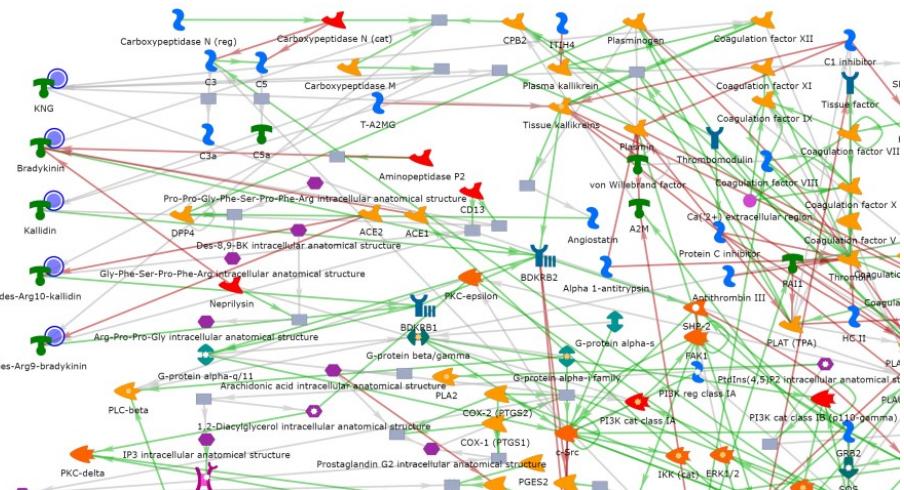
Figure 11. Process network Inflammation_Kallikrein-kinin system identified by MetaCore software from the list of differentially expressed genes (FDR 10%) in the liver of pigs fed with two different levels of soybean oil in the diet (1.5 % and 3.0 % of soybean oil). Green arrows indicates positive interactions, red arrows indicates negative interaction and gray arrows indicates unspecified interaction. For a detailed definition, see https://portal.genego.com/legends/MetaCoreQuickReferenceGuide.pdf.

4. Discussion

4.1 Different levels of dietary soybean oil modulates fat deposition: We identified differences between diets with different addition of soybean oil. The inclusion of oil in the diet did not affect growth performance and carcass traits as shown in a previous study [31]. Alencar et al. [28] and other studies revealed that soybean oil modulates FA composition in gilts in pork.

Both n-6 and n-3 PUFAs decreased as the amount of oil inclusion increased in both intramuscular fat and liver. The PUFA n-3 presented a fundamental role in the development and maintenance in the healthy animal and its ingestion is related to action effects of insulin, neurologic development, reproduction, innate and acquired immunity and with transcription factors expression [41]. In a study with *longissimus dorsi* muscle samples from pigs receiving a diet enriched with linseed (rich in AL), in the growing and finishing [41] identified genes annotated as involved in apoptosis, muscle organs development and transcriptional regulation. Beyond genes involved in the metabolic process of glicose, aminoacid metabolism, the quinase IκB cascade *NF-κB*, FA metabolic process, IGF-1/insulin and of genes that code for Wnt pathway elements. As in Alencar et al. [28] regardless of the amount of soybean oil adopted, the values were above the recommended (ratio <4:1). Values of n-6:n-3 ratio above the recommended are related to pro-inflammatory immune responses, and metabolic diseases.

The SFA and MUFA in the pigs have in vivo synthesis with low influence by diet [42], which can be observed in our results in which SFA did not present changes with the modification between oil, like the MUFA C20:1. Regarding MUFA we identified a difference in both intramuscular fat and liver, the diet is responsible for a considerable amount of OA in the adipose tissue. The *de novo* synthesis is the main one in the supply of MUFA to the body, so the tissue content is not so influenced by the diet.

Most serum parameters showed no difference with the addition of soybean oil to the diet as shown in our previous study [32]. With the increase in oil, we observed lower values of albumin, triglycerides and VLDL. In the DEG identified in Table S2, we observed APOO with higher expression (log2 fold change +0.60) in SOY1.5 encoded protein associated with HDL, LDL and VLDL lipoproteins [40], alterations in members of the apolipoprotein family may result in changes in the regulation of particle metabolism; as VLDL which may be related to the higher VLDL content found in SOY1.5.

4.2 *Different levels of dietary soybean oil modulates gene expression in skeletal muscle:* The *AL3A2* gene is present in most enriched pathway maps, both in normal and pathologically related pathways. The AL3A2 enzyme helps to detoxify aldehydes produced by alcohol metabolism and lipid peroxidation, the development of the central and peripheral nervous systems, and the oxidation of long-chain aliphatic aldehydes to fatty acid [40]. Previous study demonstrated that the *AL3A2* gene participates in the oxidation of 12-oxo-dodecanoic acid to dodecanedioic acid through the activation effect by the catalysis mechanism [43]. This gene also participates in the "leukotriene 4 biosynthesis and metabolism" pathway, where the Leukotriene E4 is formed by a family of inflammatory lipid mediators and synthesized from arachidonic acid through a diversity of cells, such as basophils, mast cells, eosinophils, and macrophages, being the final step of inactivation in "leukotriene B4 metabolism" [44]. Furthermore, *AL3A2* gene is involved in "triacylglycerol metabolism" and "oxidative stress in adipocyte dysfunction in type 2 diabetes and metabolic syndrome X" pathway, in which the accumulation of oxidative products occurs due to an imbalance in the net levels of reactive oxygen species (ROS) in relation to the antioxidant capacity of the body [45]. The different levels of soybean oil in the diet could be affecting the *AL3A2* expression level. With the increase of soybean oil in the diet, an increase in *AL3A2* occurs. Thus, the

consumption of higher levels of soybean oil could improve the rate of lipid oxidation, accumulation of free radicals into the cells causing cell damage and, consequently, the inflammatory condition that would lead to metabolic diseases such as type 2 diabetes and atherosclerosis [46]. These results confirm previous studies that identified the fatty aldehyde dehydrogenase isozymes, such as *AL3A2* have cell-specific functions associated to inflammation, differentiation, or oxidative stress responses [47,48].

The DEG *AZGP1* as observed increases with increasing dietary oil inclusion, is related to stimulation of the breakdown of lipids within adipocytes, which causes fat to be lost in some advanced cancers, and it is also capable of binding to polyunsaturated fatty acids [49]. Studies shown that the *AZGP1* gene can be inhibited by *TNF-alpha* and other genes related to the development of metabolic disorders. Also, this gene encodes a soluble protein classified as an adipokine [50,51]. In an obese adipose tissue, the overexpression of *TNF-alpha* together with IL-1b activates the ERK1/2 pathways leading to impaired gene expression that are involved in inflammation, FA oxidation, lipolysis, lipogenesis in addition to oxidative stress [52]. Our studies corroborating with previous nutrigenomics studies which showed that the *AZGP1* expression level can be affected by the diet [53,54]. The *AZGP1* gene plays a fundamental role in lipid metabolism and others metabolic diseases such as cancer, being considered as a lipid-metabolizing factor (HIRAI et al., 1998) that impacts the fatty acid metabolism, increasing lipolysis process and decreasing the inflammation signs [55,56]. According to our findings, the AZGP1 gene-enriched pathway in the skeletal muscle is directly related to dyslipidemia, inflammatory response mediated by TNF-alpha and IL-1b, and metabolic diseases.

The *CD4* gene as down-regulated DEG in skeletal muscle of pigs fed with lower level of soybean oil (SOY1.5). As well as facilitating T-cell activation, *CD4* is an important mediator of indirect neuronal damage in infections and immune-mediated conditions affecting the nervous system. Studies have been shown that diet-induced obesity increases the expression of T-cell and MHC II molecules in adipose tissue and fat spots in this tissue [57]. Skeletal muscle is an important organ for insulin response, thus, presents a significant contribution in systemic insulin sensitivity [58]. Hong et al. [59] suggested that the obesity condition affects the inflammatory state of skeletal muscle. Corroborating, Varma et al. [60], showed that diets with high level of fat can induce obesity inflammation by the macrophage infiltration into skeletal muscle. However, dietary intake of specific PUFA can modulate the inflammatory responses that can be explained by the influence of the dietary fatty acid profile into n-6:n-3 PUFA ratio of the membrane phospholipids. The n-6 PUFA metabolism generates lipid mediators that have pro-inflammatory functions while n-3 has an anti-inflammatory effect [61–63]. Therefore, the overexpression of lipid mediators generated by n-6 are associated with inflammatory diseases [61–63]. These previous findings corroborate with our results.

4.3 *Soybean oil added to pig's diet modulates gene expression in liver tissue:* The results obtained through the enriched pathways are related to the importance of the liver as a central organ for systemic metabolism [64]. Some pathways have been enriched and are important signaling pathways associated with disease. that help to understand the mechanism of genes altered by diet. The liver plays a fundamental role in the energy balance of the entire body, removes toxins such as ammonia and is responsible for the detoxification of most endogenous and exogenous toxic compounds. When some hepatic mechanism fails, it causes problems that can reach the brain, affecting brain function and causing several neurodegenerative diseases including Huntington's and AD [65,66].

In HD the majority of symptoms are related to neuronal damage although additional peripheral tissue abnormalities such as energy metabolism deficiency, skeletal muscle atrophy and adipose tissue dysfunction have been reported in both humans and

mice with HD [67]. This relationship may explain the findings in the liver of protein-coding genes with functions associated with neuronal balance. In mice, the aggregates of the resultant mutant Htt protein (mHtt) were found from the transgenic mouse model, mHtt is related with the suppression of the transcription factor *C/EBPα* (TF critical for energy homeostasis) and the *PPARγ* protein function, there is an evidence that defects in liver function may contribute to peripheral abnormalities in HD mice [67].

The *BAG-1*, which has increased expression in the SOY1.5 group, is a protein-coding gene, which is involved in binding to the membrane protein *BCL2*, which participates in the regulation of apoptosis, oncogenesis, neuronal differentiation and the reactions of cellular regulatory proteins, including glucocorticoid receptor [68]. *BAG-1* when associated with *BCL2*, it acts activating the degradation of the Huntingtin mutation, probably via activation of U-box containing protein 1 (CHIP) and proteasome [68]. Members of the *BAG* and *CHIP* family may also play an important role in modulating neurodegeneration by targeting misfolded mutant proteins to the ubiquitin-proteasome system [69]. *BAG-1* is a co-chaperone for HSP70 and HSC70 chaperone proteins, that participates as a nucleotide exchange factor (NEF) promoting ADP release from HSP70 and HSC70 proteins [40]. The HPS70 plays a protective role in several different models of nervous system injury, although it has an association with a deleterious role in some diseases [70]. Pathologies related to misfolded proteins affect different classes of neurons and are related to numerous diseases such as Parkinson disease, AD, amyotrophic lateral sclerosis (ALS), and inheritable polyglutamine (PolyQ) diseases [70]. In the study by Nollen et al. [71], with mammalian tissue culture cell lines, *BAG-1* participates as an inhibitor of Hsp70-dependent refolding the authors showed that a two-fold increase in cellular levels of *BAG-1* can inhibit Hsp70 refolding. Adrie et al. [72] showed that *BAG-1*, *BAG-3*, cellular inhibitor of apoptosis 1 (cIAP1) and myeloid cell leukemia sequence 1 (MCL-1) were more expressed in brain-dead patients than in hip surgery patients, demonstrating an inhibition of the apoptosis process. The study by Sroka et al. [68], demonstrated that BAG-1 plays a key role in neuronal survival and differentiation, and is essential for the proper development and maintenance of the central nervous system. In disease-related pathways, BAG-1 has its function compromised and this causes BAG-1 accumulation as in the enriched pathway "HSP70 and HSP40-dependent folding in Huntington's disease", which in the SOY1.5 group with higher expression would lead to even more in ubiquitin-proteasome activation, but that with HD disease, proteasome functionality is impaired and with impairment of proteasome function, it leads to changes in neurotransmitter systems [73].

On the other hand, the ST13 or Hip co-chaperone showed lower expression in the SOY1.5 group, this gene encoding the HSP70 interaction protein, which can also collaborate with other positive cofactors, such as the organizer protein HSP70-HSP90 (Hop), or compete with negative cofactors such as *BAG-1* [74]. The *ST13* can also act as a facilitator of the Hsc/HSP70 chaperone, aiding in protein folding and repair, and controlling the activity of proteins responsible for regulation, such as steroid receptors and regulators of proliferation or apoptosis [74]. According to Hou et al. [75], in case of functional alteration of the *ST13* gene, the HSP70 protein can lose control over the apoptosis process, and thus generate an incorrect proliferation. Freitas et al. [76], studying miRNA and mRNA expression in peripheral blood cells, found miR-107 down-regulated and its target the *ST13* mRNA, showing high expression in patients with high platelet reactivity. miR-107 is associated with expression inhibition of genes involved in metabolism, cell division, angiogenesis and stress response [77], and has been associated with neurodegenerative diseases and cancer [77]. In the SOY1.5 group, the expression was lower, decreasing its ability to prevent the newly formed Hsc/Hsp70-substrate

complex from prematurely dissociating in the "HSP70 and HSP40-dependent folding in Huntington's disease" pathway.

The *Tau/MAPT* was also enriched in the "Tau pathology in Alzheimer disease" pathway together with protein phosphatase, PPM1F identified in the pathway as the PP2C group with the highest expression in the SOY1.5 group. *PPM1F* phosphatase dephosphorylates and negatively regulates the activities of MAP kinases, in addition to being able to interact with guanine Rho nucleotide exchange factors [78]. The AD is characterized by the extracellular accumulation of amyloid beta peptides or plaques (Aβ) and the intracellular accumulation of phosphorylated tau protein species (tau tangles) in the brain. The Hsp-70/Hsc-70 chaperone, mentioned above, can bind to the *Tau/MAPT* protein, reducing its phosphorylation and inducing its proteasomal degradation. In addition, Hsp-70 is involved in mediating the degradation of Tau/MAPT by recruiting the CHIP E3 ubiquitin ligase, whereas *BAG-1* can associate with *Tau/MAPT* in a Hsc-70-dependent manner and inhibit its proteasomal degradation [79,80]. In the study by Elliott; Laufer; Ginzburg, [80] in AD hippocampi, the authors reported that *BAG-1* co-localizes with both tau tangles and intracellular amyloid which may indicate that BAG-1 plays a significant role in AD pathology.

As Tau (MAPT) are the proteins that stabilize microtubules, the SOY1.5 group was less expressed, thus potentiating the non-stabilization of microtubules, which is harmful. Duan et al. [81] suggested that the abnormal hyperphosphorylation of *Tau/MAPT* is caused by the conformational change of this protein in the diseased brain, making this a favorable environment for phosphorylation or an unfavorable one for dephosphorylation. Neurodegenerative disease such as AD is characterized by the microtubule-associated neuronal protein *MAPT* that undergoes hyperphosphorylation by multiple kinases resulting in microtubule disintegration, and this phosphorylation can be regulated by several phosphatases including *PP2C* [78]. In the study by Liu et al. [78] with several pools of Tau proteins isolated from AD brain, observed that Tau is abnormally hyperphosphorylated and glycosylated when there is an imbalance between phosphorylation and dephosphorylation, favoring the formation of intraneuronal neurofibrillary tangles (NFTs) which is one of the histopathology's characteristics of AD. Thus, the authors suggested that tau glycosylation is an early abnormality that facilitates hyperphosphorylation in the AD brain [78]. *I*n the "inhibition of remyelination in multiple sclerosis: regulation of cytoskeleton proteins", *MAPT* in which Fyn suppression inactivates the guanine nucleotide exchange factor Vav 2 via *CDC42*, destabilizing the actin microfilaments. Fyn suppresses glucocorticoid receptor DNA binding factor 1 leading to RhoA activation. This suppression of Fyn also impairs the interaction with *Tau (MAPT)* and alpha tubulin [82]. In the "inhibition of remyelination in multiple sclerosis: regulation of cytoskeleton proteins" RhoA binds to protein kinase 2 (ROCK2), which contains association with Rho and promotes phosphorylation and activation of protein phosphatase 1 (MLCP (reg))/protein phosphatase 1, isoenzyme beta (MLCP) (cat)), with dephosphorylation of Myosin II regulatory light chains (MRLC and MELC) [83,84]. This activation of RhoA can lead to a growth-related inhibition of the oligodendrocyte process and impair remyelination in multiple sclerosis [40].

The neurodegenerative diseases can be involved in the intracellular Ca2+ both by its lose by homeostase and excitotoxicity [85]. An overload of intracellular Ca2+ high concentration reflect in an overload of the UCP2 and UCP3 pathway in the mitochondrial Ca2+, which can induce the depolarization of the mitochondrial membrane and, as one of the consequences, activate the production of reactive oxygen-species (ROS) and stimulate the MPTP complex by the Cardiolipin/ANT pathways in PPIF [86,87].

The expression of *p21* is controlled by the *p53* tumor suppressor protein that in response to stress stimuli mediates the *p53*-dependent cell cycle G1 phase [40]. Huntingtin mutation can either activate or decrease *p53* activity and an inhibition of p53 in the "mitochondrial dysfunction in neurodegenerative diseases" pathway can lead to *p21* under expression, leading to inhibition of neuronal cell survival [88]. The gene expression analysis performed in transgenic mice with fatty livers in the study by Yahagi et al. [89], resulted in increased expression of *p21* mRNA, considered an indicator of *p53* activity. Thus, the cellular toxicity of excess FFA, lipid peroxidation and oxidative stress may be associated with the mechanisms of activation of the *p53* protein [89].

Bradykinin plays an important role in mediating inflammation resulting in vasodilation in addition to stimulating prostaglandin synthesis (Bennett, 2007). Process networks were related to both the chaperone group (HSP90) and pro-inflammatory activity, respectively. These results from the gene networks corroborate with the pathway maps shown above, highlighting that the change in the amount of oil in the diet of male pigs causes a change in the gene expression.

4.4 Genes common to dietary treatments and overview of the effect of soybean oil addition in different tissues: By identifying the common genes between the tissues, we observed the influence on modulation and important relationship to Cell cycle related kinase, in addition to the relationship to the Ca, cAMP and lipid signaling pathways and glycosylation.

As observed and discussed regarding the genes that showed differential expression, we observed a better relationship when using SOY3.0 associated with the enriched pathways presented and the association with gene function. In liver tissue we identified 45 DEG and relation to neurodegenerative diseases, which highlights the importance of the liver in disease regulation. In contrast, in skeletal muscle 281 DEG were identified with greater relation to FA metabolism, metabolic diseases and inflammatory processes. Our findings show similar function signaling pathways and networks and DEG with respect to the changes that were obtained by modulating the FA profile, making an important contribution to nutrigenomics studies.

The main processes involved are related to the immune response and inflammation, again we observe the DEG that have relation to important genes and that can modulate several processes, both in muscle and in the liver.

5. Conclusions

In this nutrigenomics study, we verified that increasing the level of soybean oil in the diet of pigs, an animal model for metabolic diseases in humans, affected the transcriptome profile of skeletal muscle and liver tissue. The differentially expressed genes identified here participate in network maps associated with metabolic and neurodegenerative diseases in pathways such as "TNF-alpha, IL-1 beta induces dyslipidemia and inflammation in obesity and type 2 diabetes in adipocytes" and "HSP70 and HSP40-dependent folding in Huntington's disease" in addition to DEGs that are related to relevant biological processes. The FA profile showed changes according to the increase in oil in the diet. These findings may help us to better understand the biological mechanisms that can be modulated through the diet, in this study specifically by increasing the level of soybean oil (an important source of unsaturated fatty acids) in the diet of pigs.

corrected *p-value* in RNA-Seq data from (A) skeletal muscle and (B) liver tissue of pigs fed with two different level of soybean oil in the diet (1.5 % and 3.0 % of soybean oil). Figure S2: Leukotriene 4 biosynthesis and metabolism pathway map created by using MetaCore software (p-value <0.10) and the list of differentially expressed genes (FDR 10%) in the skeletal muscle of pigs fed with two different levels of soybean oil in the diet (1.5 % and 3.0 % of soybean oil). The blue thermometer indicates that the DEG is down-regulated (log2 fold change -0.77) in the diet with 1.5 % of soybean oil (SOY1.5). Green arrows indicates positive interaction and gray arrows indicates unspecified interaction. For a detailed definition, see https://portal.genego.com/legends/MetaCoreQuickReferenceGuide.pdf. Figure S3: Triacylglycerol metabolism p.1 pathway map created by using MetaCore software (*p-value* <0.10) and the list of differentially expressed genes (FDR 10%) in the skeletal muscle of pigs fed with two different levels of soybean oil in the diet (1.5 % and 3.0 % of soybean oil). The blue thermometer indicates that the DEG is down-regulated (log2 fold change -0.77) in the diet with 1.5 % of soybean oil (SOY1.5). Green arrows indicates polog2 fold changesitive interaction and gray arrows indicates unspecified interaction. For a detailed definition, see https://portal.genego.com/legends/MetaCoreQuickReferenceGuide.pdf. Figure S4: Oxidative stress in adipocyte dysfunction in type 2 diabetes and metabolic syndrome X pathway map created by using MetaCore software (p-value <0.10) and the list of differentially expressed genes (FDR 10%) in the skeletal muscle of pigs fed with two different levels of soybean oil in the diet (1.5 % and 3.0 % of soybean oil). The blue thermometer indicates that the DEG is down-regulated (log2 fold change -0.77) in the diet with 1.5 % of soybean oil (SOY1.5). A green arrow indicates positive interactions; a red arrow indicates negative interaction and gray arrows indicates unspecified interaction. For a detailed definition, see https://portal.genego.com/legends/MetaCoreQuickReferenceGuide.pdf. Figure S5: Peroxisomal branched chain fatty acid oxidation pathway map created by using MetaCore software (p-value <0.10) and the list of differentially expressed genes (FDR 10%) in the skeletal muscle of pigs fed with two different levels of soybean oil in the diet (1.5 % and 3.0 % of soybean oil). The blue thermometer indicates that the DEG is down-regulated (log2foldchange -0.77) in the diet with 1.5 % of soybean oil (SOY1.5). A green arrow indicates positive interaction and gray arrows indicates unspecified interaction. For a detailed definition, see https://portal.genego.com/legends/MetaCoreQuickReferenceGuide.pdf. Figure S6. Mitochondrial dysfunction in neurodegenerative diseases pathway map created by using MetaCore software (p-value <0.10) and the list of differentially expressed genes (FDR 10%) in the liver of pigs fed with two different levels of soybean oil in the diet (1.5 % and 3.0 % of soybean oil). The red thermometer indicates that the DEG is up-regulated (log2 fold change +0.81 and +0.57) in the diet with 1.5 % of soybean oil (SOY1.5). Purple lines indicatess enhances in diseases and purple dotted line emerges in diseases. Green arrows indicates positive interactions, red arrows indicate negative interactions and grey arrows indicates unspecified interactions. For a detailed definition, see https://portal.genego.com/legends/MetaCoreQuickReferenceGuide.pdf.

Table S1: Mapped reads Sscrofa11.1 reference genome assembly. Table S2a: Differently expressed genes identified between the two groups of animals that were fed with diets enriched with different levels of soybean oil in skeletal muscle. Table S2b: Differently expressed genes identified between the two groups of animals that were fed with diets enriched with different levels of soybean oil in liver.

References

1.   World Health Organization Europe WHO/Europe | Noncommunicable diseases.
2.   Litten-Brown, J.C.; Corson, A.M.; Clarke, L. Porcine models for the metabolic syndrome, digestive and bone disorders: A general overview. *Animal* **2010**, *4*, doi:10.1017/S1751731110000200.
3.   Hao, Y.; Xing, M.; Gu, X. Research progress on oxidative stress and its nutritional regulation strategies in pigs. *Animals* 2021, *11*.
4.   Pan, Z.; Yao, Y.; Yin, H.; Cai, Z.; Wang, Y.; Bai, L.; Kern, C.; Halstead, M.; Chanthavixay, G.; Nares, T.; et al. Pig genome functional annotation enhances the biological interpretation of complex traits and human disease. *Nat Commun* **2021**, *12*, doi:https://doi.org/10.1038/s41467-021-26153-7.
5.   Malgwi, I.H.; Halas, V.; Grunvald, P.; Schiavon, S.; Jocsak, I. Genes Related to Fat Metabolism in Pigs and Intramuscular Fat Content of Pork: A Focus on Nutrigenetics and Nutrigenomics. *Animals* **2022**.
6.   Li, Y.R.; Trush, M. Defining ROS in Biology and Medicine. *React. Oxyg. Species* **2016**, *1*, doi:10.20455/ros.2016.803.
7.   Lobo, V.; Patil, A.; Phatak, A.; Chandra, N. Free radicals, antioxidants and functional foods: Impact on human health. *Pharmacogn. Rev.* 2010, *4*.
8.   Laaksonen, D.E.; Nyyssönen, K.; Niskanen, L.; Rissanen, T.H.; Salonen, J.T. Prediction of cardiovascular mortality in middle-aged men by dietary and serum linoleic and polyunsaturated fatty acids. *Arch. Intern. Med.* **2005**, *165*, doi:10.1001/archinte.165.2.193.
9.   Lunney, J.K. Advances in swine biomedical model genomics. *Int. J. Biol. Sci.* 2007, *3*.
10.   Malgwi, I.H.; Halas, V.; Grünvald, P.; Schiavon, S.; Jócsák, I. Genes Related to Fat Metabolism in Pigs and Intramuscular Fat Content of Pork: A Focus on Nutrigenetics and Nutrigenomics. **2022**, doi:10.3390/ani12020150.
11.   Kragh, P.M.; Nielsen, A.L.; Li, J.; du, Y.; Lin, L.; Schmidt, M.; Bøgh, I.B.; Holm, I.E.; Jakobsen, J.E.; Johansen, M.G.; et al. Hemizygous minipigs produced by random gene insertion and handmade cloning express the Alzheimer's disease-causing dominant mutation APPsw. *Transgenic Res.* **2009**, *18*, doi:10.1007/s11248-009-9245-4.
12.   Reddy, A.M.; Zheng, Y.; Jagadeeswaran, G.; Macmil, S.L.; Graham, W.B.; Roe, B.A.; Desilva, U.; Zhang, W.; Sunkar, R. Cloning, characterization and expression analysis of porcine microRNAs. *BMC Genomics* **2009**, *10*, doi:10.1186/1471-2164-10-65.
13.   Ramayo-Caldas, Y.; Mach, N.; Esteve-Codina, A.; Corominas, J.; Castelló, A.; Ballester, M.; Estellé, J.; Ibáñez-Escriche, N.; Fernández, A.I.; Pérez-Enciso, M.; et al. Liver transcriptome profile in pigs with extreme phenotypes of intramuscular fatty acid composition. *BMC Genomics* **2012**, *13*, doi:10.1186/1471-2164-13-547.
14.   Son, Y.; Paton, C.M. Lipid metabolic features of skeletal muscle in pathological and physiological conditions. In *Lipid Signaling and Metabolism*; Academic Press, 2020; pp. 359–383.
15.   Di Cara, F.; Andreoletti, P.; Trompier, D.; Vejux, A.; Bülow, M.H.; Sellin, J.; Lizard, G.; Cherkaoui-Malki, M.; Savary, S. Peroxisomes in immune response and inflammation. *Int. J. Mol. Sci.* **2019**, *20*, doi:10.3390/ijms20163877.
16.   Bernardi, S.; Marcuzzi, A.; Piscianz, E.; Tommasini, A.; Fabris, B. The complex interplay between lipids, immune system and interleukins in cardio-metabolic diseases. *Int. J. Mol. Sci.* 2018, *19*.
17.   Hotamisligil, G.S. Foundations of Immunometabolism and Implications for Metabolic Health and Disease. *Immunity*

2017, _47_.

18.   Nakamura, M.T.; Nara, T.Y. Essential fatty acid synthesis and its regulation in mammals. _Prostaglandins, Leukot. Essent. Fat. Acids_ **2003**, _68_, 145–150, doi:10.1016/S0952-3278(02)00264-8.

19.   Wood, J.D.; Enser, M.; Fisher, A. V.; Nute, G.R.; Sheard, P.R.; Richardson, R.I.; Hughes, S.I.; Whittington, F.M. Fat deposition, fatty acid composition and meat quality: A review. _Meat Sci._ **2008**, _78_, 343–358, doi:10.1016/j.meatsci.2007.07.019.

20.   Schwingshackl, L.; Hoffmann, G. Association of dietary, circulating, and supplement fatty acids with coronary risk 2014, 455–6.

21.   Cesar, A.S.M.; Regitano, L.C.A.; Poleti, M.D.; Andrade, S.C.S.; Tizioto, P.C.; Oliveira, P.S.N.; Felício, A.M.; do Nascimento, M.L.; Chaves, A.S.; Lanna, D.P.D.; et al. Differences in the skeletal muscle transcriptome profile associated with extreme values of fatty acids content. _BMC Genomics_ **2016**, _17_, doi:10.1186/s12864-016-3306-x.

22.   Schmid, A. The role of meat fat in the human diet. _Crit. Rev. Food Sci. Nutr._ **2011**, _51_, doi:10.1080/10408390903044636.

23.   Kritchevsky, D. Antimutagenic and some other effects of conjugated linoleic acid. _Br. J. Nutr._ 2000, _83_.

24.   Terés, S.; Barceló-Coblijn, G.; Benet, M.; Álvarez, R.; Bressani, R.; Halver, J.E.; Escribá, P. V. Oleic acid content is responsible for the reduction in blood pressure induced by olive oil. _Proc. Natl. Acad. Sci. U. S. A._ **2008**, _105_, doi:10.1073/pnas.0807500105.

25.   Pauwels, E.K.J. The protective effect of the mediterranean diet: Focus on cancer and cardiovascular risk. _Med. Princ. Pract._ 2011, _20_.

26.   Tsimikas, S.; Reaven, P.D. The role of dietary fatty acids in lipoprotein oxidation and atherosclerosis. _Curr. Opin. Lipidol._ **1998**, _9_, doi:10.1097/00041433-199808000-00003.

27.   Park, J.C.; Kim, S.C.; Lee, S.D.; Jang, H.C.; Kim, N.K.; Lee, S.H.; Jung, H.J.; Kim, I.C.; Seong, H.H.; Choi, B.H. Effects of dietary fat types on growth performance, pork quality, and gene expression in growing-finishing pigs. _Asian-Australasian J. Anim. Sci._ **2012**, _25_, doi:10.5713/ajas.2012.12416.

28.   Alencar, S.A. da S.; Kiefer, C.; Nascimento, K.M.R. de S.; Viana, L.H.; Corassa, A.; Gomes, M. de N.B.; Marçal, D.A.; Farias, T.V.A. Dietary soybean oil modulates fatty acid composition of pork. _Trop. Anim. Health Prod._ **2021**, _53_, doi:10.1007/s11250-021-02804-1.

29.   Fass _Guide for the care and use of agricultural animals in research and teaching_; 2010;

30.   Fujii, J.; Otsu, K.; Zorzato, F.; De Leon, S.; Khanna, V.K.; Weiler, J.E.; O'Brien, P.J.; Maclennan, D.H. Identification of a mutation in porcine ryanodine receptor associated with malignant hyperthermia. _Science (80-.)._ **1991**, _253_, doi:10.1126/science.1862346.

31.   Almeida, V. V.; Silva, J.P.M.; Schinckel, A.P.; Meira, A.N.; Moreira, G.C.M.; Gomes, J.D.; Poleti, M.D.; Dargelio, M.D.B.; Patinho, I.; Contreras-Castillo, C.J.; et al. Effects of increasing dietary oil inclusion from different sources on growth performance, carcass and meat quality traits, and fatty acid profile in genetically lean immunocastrated male pigs. _Livest. Sci._ **2021**, _248_, 104515, doi:10.1016/j.livsci.2021.104515.

32.   Fanalli, S.L.; Silva, B.P.M. da; Gomes, J.D.; Almeida, V.V. de; Afonso, J.; Reecy, J.M.; Koltes, J.E.; Koltes, D.; Balieiro, J.C. de C.; Freitas, L.; et al. Effect of Dietary Soybean Oil Inclusion on Liver-Related Transcription Factors in a Pig Model for Metabolic Diseases 2022.

33.   Rostagno, H.S. Tabelas brasileiras para aves e suínos: composição de alimentos e exigências nutricionais. _Tabelas Bras. para aves e suínos Compos. Aliment. e Exig. Nutr._ **2011**.

34.   BLIGH, E.G.; DYER, W.J. A rapid method of total lipid extraction and purification. _Can. J. Biochem. Physiol._ **1959**, _37_, doi:10.1139/o59-099.

35.   AOCS Official approved procedure Am 5-04, Rapid determination of oil/fat utilizing high temperature solvent extraction. _Am. Oil Chem. Soc._ **2005**.

36.   Love, M.I.; Huber, W.; Anders, S. Moderated estimation of fold change and dispersion for RNA-seq data with DESeq2. _Genome Biol._ **2014**, _15_, doi:10.1186/s13059-014-0550-8.

37.   Benjamini, Y.; Hochberg, Y. Controlling the False Discovery Rate: A Practical and Powerful Approach to Multiple Testing. _J. R. Stat. Soc. Ser. B_ **1995**, _57_, doi:10.1111/j.2517-6161.1995.tb02031.x.

38.   MetaCore (Clarivate Analytics) 2021.

39.   Malumbres, M. Cyclin-dependent kinases. _Genome Biol._ **2014**, _15_, doi:10.1186/gb4184.

40.   Stelzer, G.; Rosen, N.; Plaschkes, I.; Zimmerman, S.; Twik, M.; Fishilevich, S.; Iny Stein, T.; Nudel, R.; Lieder, I.; Mazor, Y.; et al. The GeneCards suite: From gene data mining to disease genome sequence analyses. _Curr. Protoc. Bioinforma._ **2016**, _2016_, doi:10.1002/cpbi.5.

41.   Wei, H.; Zhou, Y.; Jiang, S.; Huang, F.; Peng, J.; Jiang, S. Transcriptional response of porcine skeletal muscle to feeding a linseed-enriched diet to growing pigs. _J. Anim. Sci. Biotechnol._ **2016**, _7_, doi:10.1186/s40104-016-0064-1.

42.   Enser, M.; Richardson, R.I.; Wood, J.D.; Gill, B.P.; Sheard, P.R. Feeding linseed to increase the n-3 PUFA of pork: Fatty acid composition of muscle, adipose tissue, liver and sausages. _Meat Sci._ **2000**, _55_, doi:10.1016/S0309-1740(99)00144-8.

43.   Kelson, T.L.; Secor McVoy, J.R.; Rizzo, W.B. Human liver fatty aldehyde dehydrogenase: Microsomal localization, purification, and biochemical characterization. _Biochim. Biophys. Acta - Gen. Subj._ **1997**, _1335_, doi:10.1016/S0304-4165(96)00126-2.

44.   Peters-Golden, M.; Gleason, M.M.; Togias, A. Cysteinyl leukotrienes: Multi-functional mediators in allergic rhinitis. _Clin._

Exp. Allergy 2006, *36*.

45. Maslov, L.N.; Naryzhnaya, N. V.; Boshchenko, A.A.; Popov, S. V.; Ivanov, V. V.; Oeltgen, P.R. Is oxidative stress of adipocytes a cause or a consequence of the metabolic syndrome? *J. Clin. Transl. Endocrinol.* 2019, *15*.

46. Pan, C.; Xing, J.H.; Zhang, C.; Zhang, Y.M.; Zhang, L.; Wei, S.J.; Zhang, M.X.; Wang, X.P.; Yuan, Q.H.; Xue, L.; et al. Aldehyde dehydrogenase 2 inhibits inflammatory response and regulates atherosclerotic plaque. *Oncotarget* **2016**, *7*, doi:10.18632/oncotarget.9384.

47. Bazewicz, C.G.; Dinavahi, S.S.; Schell, T.D.; Robertson, G.P. Aldehyde dehydrogenase in regulatory T-cell development, immunity and cancer. *Immunology* 2019, *156*.

48. Chu, A.; Najafzadeh, P.; Sullivan, P.; Cone, B.; Elshimali, R.; Shakeri, H.; Janzen, C.; Mah, V.; Wadehra, M. Aldehyde dehydrogenase isoforms and inflammatory cell populations are differentially expressed in term human placentas affected by intrauterine growth restriction. *Placenta* **2019**, *81*, doi:10.1016/j.placenta.2019.03.015.

49. Krahmer, N.; Farese, R. V.; Walther, T.C. Balancing the fat: Lipid droplets and human disease. *EMBO Mol. Med.* 2013, *5*.

50. Gohda, T.; Makita, Y.; Shike, T.; Tanimoto, M.; Funabiki, K.; Horikoshi, S.; Tomino, Y. Identification of epistatic interaction involved in obesity using the KK/Ta mouse as a type 2 diabetes model: Is Zn-α2 glycoprotein-1 a candidate gene for obesity? *Diabetes* **2003**, *52*, doi:10.2337/diabetes.52.8.2175.

51. Tzanavari, T.; Bing, C.; Trayhurn, P. Postnatal expression of zinc-α2-glycoprotein in rat white and brown adipose tissue. *Mol. Cell. Endocrinol.* **2007**, *279*, doi:10.1016/j.mce.2007.08.015.

52. Jager, J.; Grémeaux, T.; Gonzalez, T.; Bonnafous, S.; Debard, C.; Laville, M.; Vidal, H.; Tran, A.; Gual, P.; Marchand-Brustel, Y. Le; et al. Tpl2 kinase is upregulated in adipose tissue in obesity and may mediate interleukin-1β and tumor necrosis factor-α effects on extracellular signal-regulated kinase activation and lipolysis. *Diabetes* **2010**, *59*, doi:10.2337/db09-0470.

53. Faulconnier, Y.; Bernard, L.; Boby, C.; Domagalski, J.; Chilliard, Y.; Leroux, C. Extruded linseed alone or in combination with fish oil modifies mammary gene expression profiles in lactating goats. *Animal* **2018**, *12*, doi:10.1017/S1751731117002816.

54. Ollier, S.; Robert-Granié, C.; Bernard, L.; Chilliard, Y.; Leroux, C. Mammary transcriptome analysis of food-deprived lactating goats highlights genes involved in milk secretion and programmed cell death. *J. Nutr.* **2007**, *137*, doi:10.1093/jn/137.3.560.

55. Choi, J.W.; Liu, H.; Mukherjee, R.; Yun, J.W. Downregulation of fetuin-B and zinc-α2-glycoprotein is linked to impaired fatty acid metabolism in liver cells. *Cell. Physiol. Biochem.* **2012**, *30*, doi:10.1159/000339065.

56. Liu, T.; Luo, X.; Li, Z.H.; Wu, J.C.; Luo, S.Z.; Xu, M.Y. Zinc-α2-glycoprotein 1 attenuates non-alcoholic fatty liver disease by negatively regulating tumour necrosis factor-α. *World J. Gastroenterol.* **2019**, *25*, doi:10.3748/wjg.v25.i36.5451.

57. Morris, D.L.; Cho, K.W.; DelProposto, J.L.; Oatmen, K.E.; Geletka, L.M.; Martinez-Santibanez, G.; Singer, K.; Lumeng, C.N. Adipose tissue macrophages function as antigen-presenting cells and regulate adipose tissue cd4+ t cells in mice. *Diabetes* **2013**, *62*, doi:10.2337/db12-1404.

58. Feraco, A.; Gorini, S.; Armani, A.; Camajani, E.; Rizzo, M.; Caprio, M. Exploring the role of skeletal muscle in insulin resistance: lessons from cultured cells to animal models. *Int. J. Mol. Sci.* 2021, *22*.

59. Hong, E.G.; Hwi, J.K.; Cho, Y.R.; Kim, H.J.; Ma, Z.; Yu, T.Y.; Friedline, R.H.; Kurt-Jones, E.; Finberg, R.; Fischer, M.A.; et al. Interleukin-10 prevents diet-induced insulin resistance by attenuating macrophage and cytokine response in skeletal muscle. *Diabetes* **2009**, *58*, doi:10.2337/db08-1261.

60. Varma, V.; Yao-Borengasser, A.; Rasouli, N.; Nolen, G.T.; Phanavanh, B.; Starks, T.; Gurley, C.; Simpson, P.; McGehee, R.E.; Kern, P.A.; et al. Muscle inflammatory response and insulin resistance: Synergistic interaction between macrophages and fatty acids leads to impaired insulin action. *Am. J. Physiol. - Endocrinol. Metab.* **2009**, *296*, doi:10.1152/ajpendo.90885.2008.

61. Calder, P.C. Fatty acids and inflammation: The cutting edge between food and pharma. In Proceedings of the European Journal of Pharmacology; 2011; Vol. 668.

62. Djuricic, I.; Calder, P.C. Beneficial outcomes of omega-6 and omega-3 polyunsaturated fatty acids on human health: An update for 2021. *Nutrients* 2021, *13*.

63. Innes, J.K.; Calder, P.C. Omega-6 fatty acids and inflammation. *Prostaglandins Leukot. Essent. Fat. Acids* 2018, *132*.

64. Horodyska, J.; Hamill, R.M.; Reyer, H.; Trakooljul, N.; Lawlor, P.G.; McCormack, U.M.; Wimmers, K. RNA-seq of liver from pigs divergent in feed efficiency highlights shifts in macronutrient metabolism, hepatic growth and immune response. *Front. Genet.* **2019**, *10*, doi:10.3389/fgene.2019.00117.

65. Carroll, J.B.; Bates, G.P.; Steffan, J.; Saft, C.; Tabrizi, S.J. Treating the whole body in Huntington's disease. *Lancet Neurol.* 2015, *14*.

66. Felipo, V. Hepatic encephalopathy: Effects of liver failure on brain function. *Nat. Rev. Neurosci.* 2013, *14*.

67. Chiang, M.C.; Chern, Y.; Juo, C.G. The dysfunction of hepatic transcriptional factors in mice with Huntington's Disease. *Biochim. Biophys. Acta - Mol. Basis Dis.* **2011**, *1812*, doi:10.1016/j.bbadis.2011.05.006.

68. Sroka, K.; Voigt, A.; Deeg, S.; Reed, J.C.; Schulz, J.B.; Bähr, M.; Kermer, P. BAG1 modulates huntingtin toxicity, aggregation, degradation, and subcellular distribution. *J. Neurochem.* **2009**, *111*, doi:10.1111/j.1471-4159.2009.06363.x.

69. Kalia, S.K.; Kalia, L. V; McLean, P.J. Molecular chaperones as rational drug targets for Parkinson's disease therapeutics.

CNS Neurol. Disord. Drug Targets **2010**, *9*, doi:10.2174/187152710793237386.

70. Geraci, F.; Turturici, G.; Sconzo, G. Hsp70 and its molecular role in nervous system diseases. *Biochem. Res. Int.* 2011.

71. Nollen, E.A.A.; Brunsting, J.F.; Song, J.; Kampinga, H.H.; Morimoto, R.I. Bag1 Functions In Vivo as a Negative Regulator of Hsp70 Chaperone Activity. *Mol. Cell. Biol.* **2000**, *20*, doi:10.1128/mcb.20.3.1083-1088.2000.

72. Adrie, C.; Monchi, M.; Fulgencio, J.P.; Cottias, P.; Haouache, H.; Alvarez-Gonzalvez, A.; Guerrini, P.; Cavaillon, J.M.; Adib-Conquy, M. Immune status and apoptosis activation during brain death. *Shock* **2010**, *33*, doi:10.1097/SHK.0b013e3181b65b99.

73. Jana, N.R.; Zemskov, E.A.; Wang, G.H.; Nukina, N. Altered proteasomal function due to the expression of polyglutamine-expanded truncated N-terminal huntingtin induces apoptosis by caspase activation through mitochondrial cytochrome c release. *Hum. Mol. Genet.* **2001**, *10*, doi:10.1093/hmg/10.10.1049.

74. Shi, Z. zheng; Zhang, J. wei; Zheng, S. What we know about ST13, a co-factor of heat shock protein, or a tumor suppressor? *J. Zhejiang Univ. Sci. B.* 2007, *8*.

75. Hou, Y.; Song, L.; Zhu, P.; Zhang, B.; Tao, Y.; Xu, X.; Li, F.; Wu, K.; Liang, J.; Shao, D.; et al. Single-cell exome sequencing and monoclonal evolution of a JAK2-negative myeloproliferative neoplasm. *Cell* **2012**, *148*, doi:10.1016/j.cell.2012.02.028.

76. Freitas, R.C.C. de; Bortolin, R.H.; Lopes, M.B.; Hirata, M.H.; Hirata, R.D.C.; Silbiger, V.N.; Luchessi, A.D. Integrated analysis of miRNA and mRNA gene expression microarrays: Influence on platelet reactivity, clopidogrel response and drug-induced toxicity. *Gene* **2016**, *593*, doi:10.1016/j.gene.2016.08.028.

77. Finnerty, J.R.; Wang, W.X.; Hébert, S.S.; Wilfred, B.R.; Mao, G.; Nelson, P.T. The miR-15/107 group of MicroRNA genes: Evolutionary biology, cellular functions, and roles in human diseases. *J. Mol. Biol.* 2010, *402*.

78. Liu, F.; Grundke-Iqbal, I.; Iqbal, K.; Gong, C.X. Contributions of protein phosphatases PP1, PP2A, PP2B and PP5 to the regulation of tau phosphorylation. *Eur. J. Neurosci.* **2005**, *22*, doi:10.1111/j.1460-9568.2005.04391.x.

79. Caecilie Signore, S.; Silvester Wouters, F.; Schmitz, M.; Baehr, M.; Kermer, P. BAG1 Overexpression Stabilizes High Molecular Tau Protein – a Crucial Role of the Co-chaperone in Tau Pathology. *Am. J. Psychiatry Neurosci.* **2021**, *9*, doi:10.11648/j.ajpn.20210902.18.

80. Elliott, E.; Laufer, O.; Ginzburg, I. BAG-1M is up-regulated in hippocampus of Alzheimer's disease patients and associates with tau and APP proteins. *J. Neurochem.* **2009**, *109*, doi:10.1111/j.1471-4159.2009.06047.x.

81. Duan, Y.; Dong, S.; Gu, F.; Hu, Y.; Zhao, Z. Advances in the Pathogenesis of Alzheimer's Disease: Focusing on Tau-Mediated Neurodegeneration. *Transl. Neurodegener.* 2012, *1*.

82. Bustelo, X.R. Regulatory and Signaling Properties of the Vav Family. *Mol. Cell. Biol.* **2000**, *20*, doi:10.1128/mcb.20.5.1461-1477.2000.

83. Baer, A.S.; Syed, Y.A.; Kang, S.U.; Mitteregger, D.; Vig, R.; Ffrench-Constant, C.; Franklin, R.J.M.; Altmann, F.; Lubec, G.; Kotter, M.R. Myelin-mediated inhibition of oligodendrocyte precursor differentiation can be overcome by pharmacological modulation of Fyn-RhoA and protein kinase C signalling. *Brain* **2009**, *132*, doi:10.1093/brain/awn334.

84. Maekawa, M.; Ishizaki, T.; Boku, S.; Watanabe, N.; Fujita, A.; Iwamatsu, A.; Obinata, T.; Ohashi, K.; Mizuno, K.; Narumiya, S. Signaling from Rho to the actin cytoskeleton through protein kinases ROCK and LIM-kinase. *Science (80-.).* **1999**, *285*, doi:10.1126/science.285.5429.895.

85. Rego, A.C.; Oliveira, C.R. Mitochondrial dysfunction and reactive oxygen species in excitotoxicity and apoptosis: Implications for the pathogenesis of neurodegenerative diseases. *Neurochem. Res.* 2003, *28*.

86. Beal, M.F. Mitochondrial dysfunction in neurodegenerative diseases. *Biochim. Biophys. Acta - Bioenerg.* **1998**, *1366*, 211–223, doi:10.1016/S0005-2728(98)00114-5.

87. Brustovetsky, N.; Brustovetsky, T.; Purl, K.J.; Capano, M.; Crompton, M.; Dubinsky, J.M. Increased susceptibility of striatal mitochondria to calcium-induced permeability transition. *J. Neurosci.* **2003**, *23*, doi:10.1523/jneurosci.23-12-04858.2003.

88. Steffan, J.S.; Kazantsev, A.; Spasic-Boskovic, O.; Greenwald, M.; Zhu, Y.Z.; Gohler, H.; Wanker, E.E.; Bates, G.P.; Housman, D.E.; Thompson, L.M. The Huntington's disease protein interacts with p53 and CREB-binding protein and represses transcription. *Proc. Natl. Acad. Sci. U. S. A.* **2000**, *97*, doi:10.1073/pnas.100110097.

89. Yahagi, N.; Shimano, H.; Matsuzaka, T.; Sekiya, M.; Najima, Y.; Okazaki, S.; Okazaki, H.; Tamura, Y.; Iizuka, Y.; Inoue, N.; et al. p53 Involvement in the pathogenesis of fatty liver disease. *J. Biol. Chem.* **2004**, *279*, doi:10.1074/jbc.M400884200.